Chapter 5
Multifunctional Radar Systems for Fighter Aircraft

David Lynch, Jr.

DL Sciences, Inc.

Carlo Kopp

Monash University

5.1 INTRODUCTION

In spite of more than a half century of improvements in radar performance and reliability, the effort required for deployment, operation, and maintenance of most radars is substantial. Furthermore, the power-aperture product is never as large as desired. The forward projected area as well as avionics weight is very costly in most fighter aircraft parameters. These parameters have motivated users, buyers, and designers to want more functions in a single radar and its complementary processing suite. As a result, most modern fighter radars are multifunctional—providing radar, navigation, landing aids, data link, and Electronic Counter Measures (ECM) functions.[1,2] The primary enabler for multifunctional radar is software-defined signal and data processing, first introduced in the mid 1970s.[3–6] Software programmability allows many radar system modes to be performed using the same RF hardware. In addition, modern navigation aids work so well that each radar mode is defined by its earth situation-geometry with almost all waveform parameters set by local earth conditions.[7,9] The modern radar often is net-centric, using and providing data to a communications network and where suitably equipped, has its own Internet protocol (IP) address.

Multifunctionality is not dependent on antenna type. In fact, the mechanically scanned AN/APG-65, 70, and 73 radars have demonstrated multifunctionality in combat.[7] However, multifunctionality is facilitated by Active Electronically Scanned Antenna (AESA) arrays. The multifunctional AESA radar in the F/A-18E/F fighter is shown with a protective cover over the array in Figure 5.1. The AESA is shaped and canted upward to aid in some modes and to minimize reflections to enemy radars.[8]

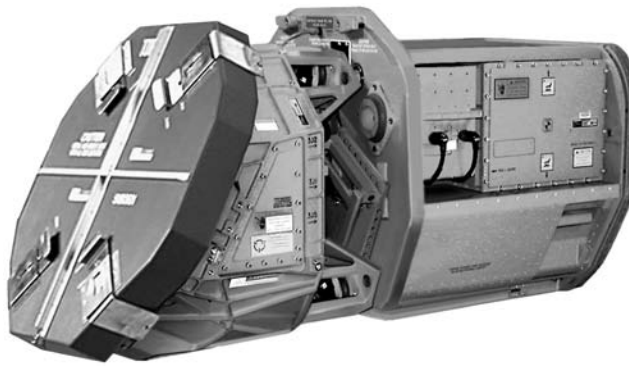

FIGURE 5.1 AN/APG-79 Multifunctional AESA Radar (*Courtesy Raytheon Company*[12])

This chapter addresses *what* signals are emitted and *why* they are needed in a Multifunctional Fighter Aircraft Radar (MFAR). The *why* begins with typical missions, which shows the geometry that gives rise to each radar mode and waveform, lists representative radar modes, and shows typical modern airborne radar mode interleaving and timing. The answer to *what* is provided by typical waveform variations and a few examples. The examples are not from any single radar but are a composite of modern radars. The general MFAR idea is illustrated in Figure 5.2. It shows time multiplexed operations for air-to-air (A-A), air-to-surface (A-S), electronic warfare (EW), and communication from the same radio frequency (RF) hardware and processing complex often over most of the microwave band.[9,11] Sometimes, multiple functions can be performed simultaneously if a common waveform is used.

The antenna aperture usually has multiple phase centers enabling measurement for Space-Time Adaptive Processing (STAP),[13] Displaced Phase Center Antenna (DPCA)

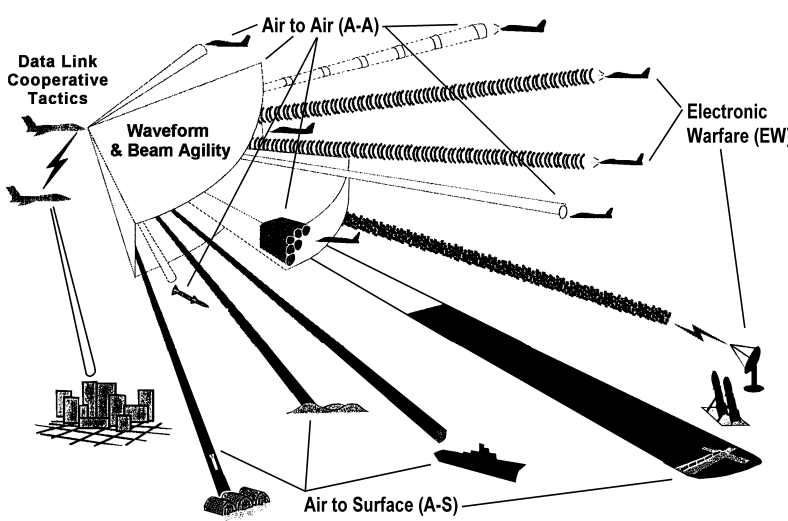

FIGURE 5.2 MFAR interleaves A-S, A-A, and EW functions (*adapted*[9])

processing, conventional monopulse angle tracking, jammer nulling, and out-of-band angle-of-arrival (AOA) estimation. The optimum placement of phase centers is an important design tradeoff. A phase center is an antenna aperture channel, which is offset in space and provides a partially or fully independent measurement of an incoming electromagnetic wavefront. For example, a one-dimensional phase monopulse has two phase centers, a two-dimensional phase monopulse has four phase centers, DPCA has two or more phase centers, a radar with a guard horn for sidelobe suppression has two phase centers, and an adaptive array may have many phase centers.[13–16] STAP is an extension of the classic theory for a matched filter in the presence of non–white noise, which includes both time and space.

Overall weapon system requirements usually favor X or K_u band for the operating frequency of a MFAR. In addition, the MFAR apertures and associated transmitter are usually the largest on an aircraft and hence, can create the highest Effective Radiated Power (ERP) for jamming adversary radars and data links, where these are in-band.

Multifunctional Radar Architecture. An example MFAR block diagram is shown in Figure 5.3. The modern integrated avionic suite concept blurs the boundaries between traditional radar functions and other sensors, countermeasures, weapons, and communications (see Figures 5.12 and 5.14 later in the chapter). There is a microwave and RF suite; an electro-optical, infrared, ultraviolet (EO) suite; a stores management suite; a controls and displays suite; a multiply-redundant vehicle management suite, and a multiply-redundant processor complex.

Each microwave and/or RF aperture may have some embedded signal conditioning but then may be multiplexed to standardized common design RF, filter, frequency reference, analog to digital conversion (A/D), input-output (I/O), and control modules. A similar design concept is used for the electro-optical (EO) sensors, stores management,

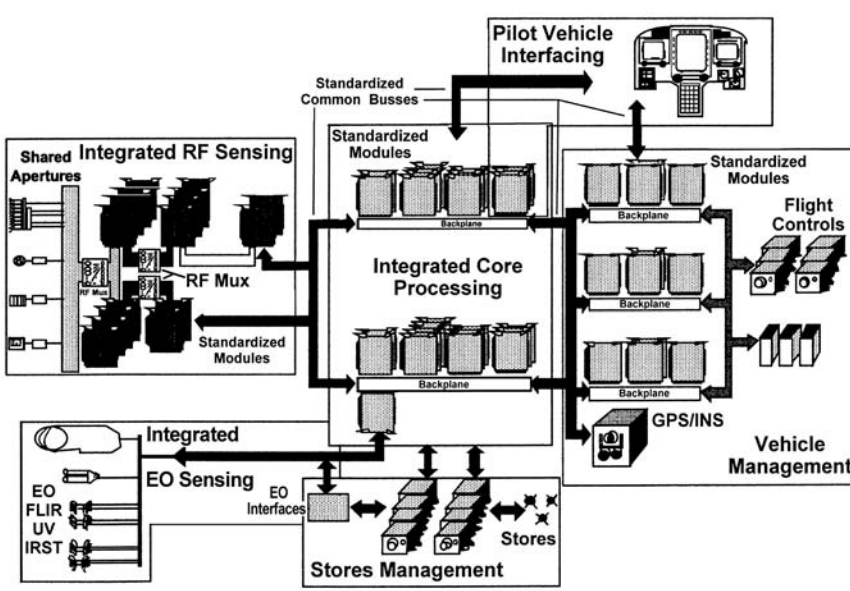

FIGURE 5.3 MFAR merged with other sensors (*adapted*[2])

vehicle management, pilot-vehicle interface, and integrated core-processing suite. There is substantial data traffic between the core processing and the sensors to provide pointing, cueing, tracking, and multisensor fusion of detections. The aim of this approach is to provide a shared pool of computational resources, which may be flexibly allocated between sensors and functions.

The sensors may contain dedicated motion sensing, but long-term navigation is provided by the vehicle management global positioning system and inertial navigation system (GPS/INS). The on-radar motion sensing must sense position to a fraction of the transmitted wavelength over the coherent processing interval. This is usually done with inertial sensors such as accelerometers and gyros with very high sampling rates. An inertial navigation system estimates the position of the aircraft in a worldwide coordinate space by integrating the outputs of the gyros and accelerometers, typically using Kalman filtering techniques. Accumulated errors in such a system can be corrected by using GPS updates as well as known reference points measured with the radar, or EO sensors.

There may be dozens or hundreds of stored program devices distributed throughout the avionics. These lower level functional suites are connected by standardized busses, which may be fiber optic or wired. The programmable devices are controlled by software operating environments invoking programs. The architecture objective is to have standard interfaces, few unique assemblies, and single-level maintenance.

The suite of microwave and RF apertures in a fighter aircraft might appear as shown in Figure 5.4. As many as 20 apertures may be distributed throughout the vehicle, performing radar, data link, navigation, missile warning, direction finding, jamming, or other functions over a frequency range covering several decades.[2] There are apertures distributed over the aircraft that point forward and aft, right and left, as well as up and down. Some apertures will be shared for communications, radio navigation, and identification (CNI) as well as identification, friend or foe (IFF) due to compatible frequencies and geometries. Data links such as JTIDS/Link 16 and Link 22 can share apertures with GPS and L band satellite communications (L SATCOM). EW apertures must be broadband by nature and can be shared with radar warning receivers (RWR), radar auxiliaries, and some types of CNIs.

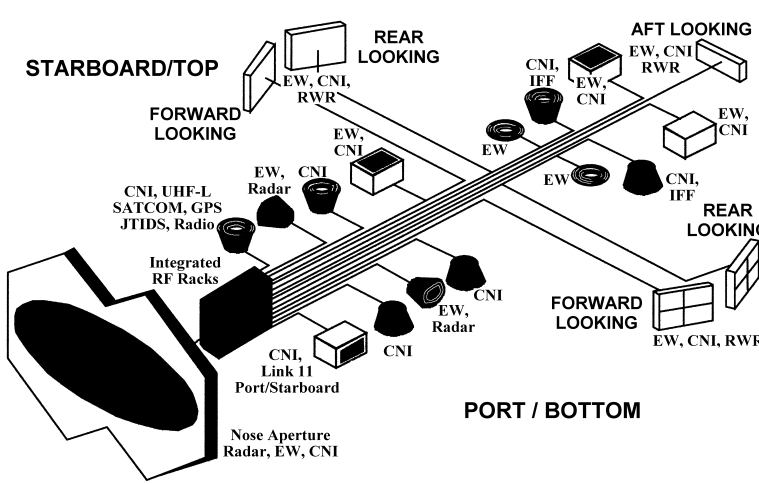

FIGURE 5.4 MFAR RF apertures share low-level RF (*adapted*[2]).

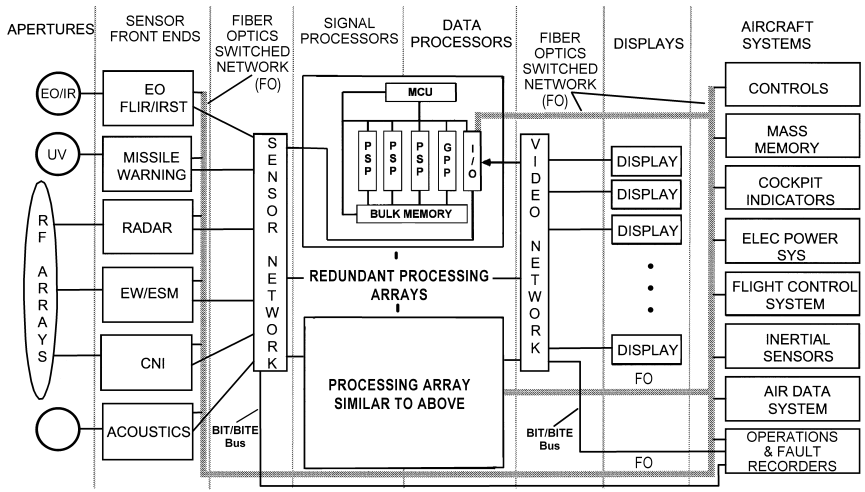

FIGURE 5.5 MFAR processing (*adapted*[2])

The apertures are signal conditioned, controlled, and interfaced through busses in the aircraft with remaining processing performed either in a common processor complex, as shown in Figure 5.5, or in federated processors distributed throughout the aircraft. One important class of standardized modules contains basic timing and programmable event generators (PEG) that create accurate timing for Pulse Repetition Frequencies (PRFs), analog to digital conversion (A/D) sampling, pulse and chip widths, blanking gates, beam repointing commands, and other synchronized real-time interrupts. A second class contains RF and intermediate frequency (IF) amplification and mixing. A third class contains low noise frequency synthesizers, which may include Direct Digital-frequency Synthesis (DDS). A/D converters and control interface modules are the final class. Bussing protocols and speeds must have adequate reserves to insure fail-safe real-time operation.

The functional block diagram and operation of a specific sensor mode is then overlaid on this hardware and software infrastructure. A specific mode is implemented in an applications program in the same sense that word-processing is on a personal computer (PC). Carrying the analogy further, common experience with the unreliability of PC hardware and software requires that a system of the type depicted in Figure 5.3 must be redundant, error checking, trusted, fail safe in the presence of faults, and embody strict program execution security. This is a very challenging system engineering task. Exhaustive mathematical assurance and system testing is required, which is completely different from current commercial personal computer practice.

A notional MFAR integrated core processing complex with its corresponding interfaces similar to that shown in Figure 5.3 is shown in Figure 5.5, where there are multiple redundant processing arrays that contain standardized modules connected in a non-blocking switched network. Internal and external busses connect the individual processing arrays to each other as well as to the other suites, sensors, controls, and displays.

Usually, there are both parallel electrical signal busses as well as serial fiber optic busses depending on speed and total length in the aircraft.[2] The signal and data processor complex contains multiple processor and memory entities, which might be

on a single chip or on separate chips depending on yield, complexity, speed, cache size, and so on. Each processor array may consist of programmable signal processors (PSP), general purpose processors (GPP), bulk memory (BM), input-output (I/O), and a master control unit (MCU). The PSPs perform signal processing on arrays of sensor data. The GPPs perform processing in which there are large numbers of conditional branches. The MCU issues programs to PSPs, GPPs, and BM, as well as manages overall execution and control. Typical processing speed is 6000 MIPS (millions of instructions per second) per chip but might be 32 GIPS (billions of instructions per second) in the near future.[17] Clock frequencies are limited by on-chip signal propagation but are up to 4 GHz (gigahertz) and could be 10 GHz in the near future.[18] Sensor processing has arrived at the point where the conception of successful algorithms is more important than the computational horsepower necessary to carry them out.

MFAR Software Structure. Improper operation of many fighter systems can be hazardous. As previously mentioned, the software must be exhaustively tested, error checked, mathematically trusted, failsafe in the presence of faults, and embody strict program execution security. One of the most important aspects is rigid adherence to a structured program architecture. An object-based hierarchical structure, where each level is subordinate to the level above and subprograms are called in strict sequence, is necessary. It also requires, among other things, that subprograms never call themselves (recursive code) or any others at their execution level. Subprograms (objects) are called, receive execution parameters from the level above (the parent), and return results back to the calling level.[94] An example of such a software structure is shown in Figures 5.6 and 5.7. The software would be executed in the hardware shown in Figure 5.5.

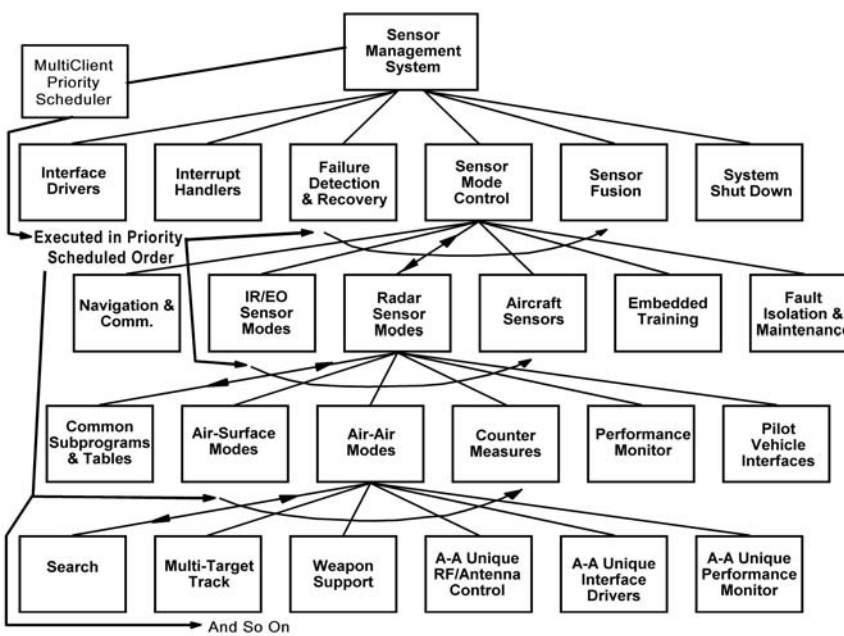

FIGURE 5.6 MFAR structured software

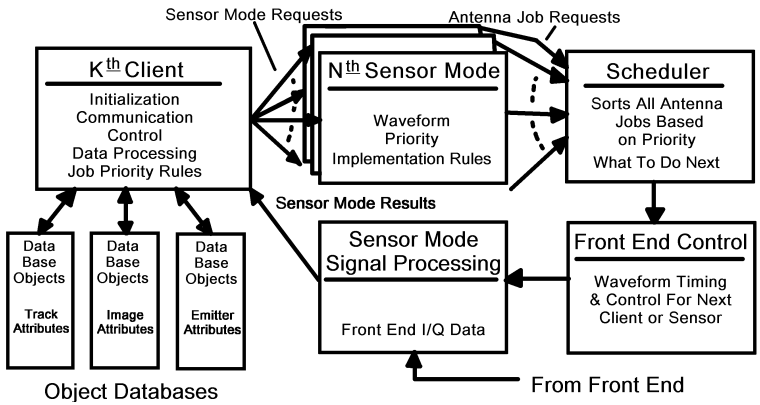

FIGURE 5.7 MFAR priority scheduling

An MFAR can support many activities (or modes) concurrently by interleaving their respective data collections. Surveillance, track updates, and ground maps are examples of such activities. The software needed to support each activity is mapped to a specific client module, as shown in Figure 5.7. Each client module is responsible for maintaining its own object database and for requesting use of the aperture. Requests are made by submitting antenna job requests that specify both the waveform to be used (how to do it) and the priority and urgency of the request.

A scheduler executes during each data collection interval and decides what to do next, based on the priorities and urgencies of the antenna job requests that have been received. This keeps the aperture busy and responsive to the latest activity requests. Following the selection of the antenna job by the scheduler, the front-end (transmit and receive) hardware is configured, and in-phase and quadriture (I/Q) data is collected and sent to the signal processors. There, the data is processed in a manner defined by the sensor mode, and the signal processing results are returned to the client that requested them. This typically results in database updates and/or new antenna job requests from the client. New activities can be added at any time using this modular approach.

Although this structure is complex and the software encompasses millions of lines of code, modern MFAR software integrity can be maintained with strict control of interfaces, formal configuration management processes, and formal verification and validation software tools. In addition, most subprograms are driven by read-only tables, as shown in Figure 5.7, so that the evolution of aircraft tactics, capabilities, and hardware do not require rewrites of validated subprograms. Software versions (builds) are updated every year throughout the lifetime of the system, which may be decades. Each subprogram must have table driven error checking as well. Many lower levels are not shown in Figures 5.6 and 5.7; there may be several thousand subprograms in all.

Range Doppler Situation. Modern radars have the luxury of interleaving most of the modes suggested in Figure 5.2 in real time and selecting the best available time or aircraft position to invoke each mode as the mission requires.[7,9]

The geometry that must be solved each time is shown in Figure 5.8. The fighter aircraft pulse doppler geometry is centered around the aircraft traveling at a velocity, V_a, and at an altitude, h, above the Earth's surface. The radar pulse repetition frequency

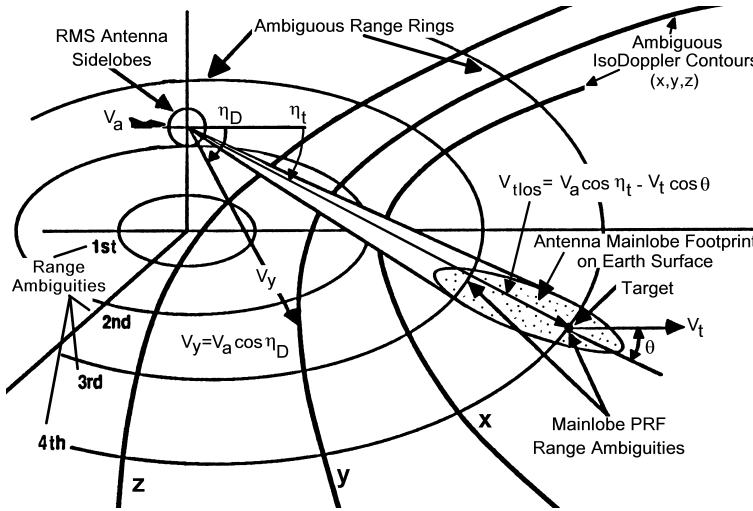

FIGURE 5.8 Strike fighter pulse doppler geometry[7,9]

(PRF) gives rise to a series of range (1, 2, 3, 4) and doppler (x, y, z) ambiguities, as shown in Figure 5.8, which intercept the Earth's surface as range "rings" and iso-doppler "hyperbolas" (because the Earth is a rough geoid, constant range and doppler contours are not actually rings or hyperbolas). The radar antenna pattern intercepts the limb of the Earth usually in both the main beam and sidelobes. A target in the main beam at range, R_t, and velocity, V_t, may have to be observed in the presence of both range and doppler ambiguities. Only the target's line-of-sight velocity, V_{tlos}, is observable on a short term basis. The radar designers' problem is to select the best waveform in this target-clutter geometry. Historically, these waveforms were selected ahead of time and built into the radar hardware and software. Most modern airborne radars solve this geometry in real time and continuously select the best available frequency, PRF, pulsewidth, transmit power, scan pattern, etc.

Unfortunately, the specifics of the waveform are unpredictable even to the radar without exact knowledge of the aircraft-target-earth velocity-geometry set and mode of operation requested by the operator or mission software. This makes testing quite difficult; fortunately, test equipment has come a long way. Hardware-in-the-loop testing using real-time simulation of the entire geometry and external world in the radar integration laboratory is commonly employed.

Active Electronically Scanned Array (AESA). Although multifunctional radars have been deployed with mechanically scanned and electronically scanned antennas, fully multifunctional radars use Active Electronically Scanned Arrays (AESA), which contain a transmit-receive channel (T/R) for each radiator.[1] The advantages of AESA are fast adaptive beam shaping and agility, improved power efficiency, improved mode interleaving, simultaneous multiple weapon support, and reduced observability.[19–23] Perhaps half the cost and complexity of an AESA is in the T/R channels. That said, however, the feed network, beam steering controller (BSC), AESA power supply, and cooling subsystem (air or liquid) are equally important.[9,11]

A major enabler for AESAs is the state of the art in microwave integrated circuits.[1] This has followed the dramatic cost and performance gains available in most semiconductor technologies. Each T/R channel has self-diagnosis features, which can detect failure and communicate that to the beam steering controller for failure compensation. AESAs can accommodate up to 10% failures with very little degradation if properly compensated in the BSC.[24]

From an MFAR point of view, the important parameters are volumetric densities high enough to support less than 1/2 wavelength spacing; radiated power densities high enough to support 4 watts per sq. cm.; radiated-to-prime-power efficiencies greater than 25%; bandwidth of several GHz on transmit and almost twice that bandwidth on receive; phase and amplitude calibration and control adequate to provide at least –50 dB rms sidelobes; amplitude control adequate to provide 50 dB power management; noise performance adequate to support the subclutter visibility requirements; and finally, sufficient storage and computing to allow beam repointing/adjustment in a fraction of 1 msec. Fast beam adjustment requires high-speed busses to each T/R channel.

One of the principal advantages of an AESA is the ability to manage both power and spatial coverage on a short-term basis (10s of msec.). Often another advantage is that both the noise figure is lower and radiated power is higher for a given amount of prime power. This is because the RF path lengths can be much shorter, which usually leads to lower front-end losses. Each radiating element is usually designed to be very broadband and is driven by a T/R channel in a typical AESA array. There are typically a few thousand channels in an MFAR AESA. Each channel contains first-level power regulation, filtering, logic, calibration tables as well as the obvious RF functions. Some channels in the array are dedicated to other functions such as calibration, jammer nulling, sidelobe blanking, close in missile datalink, out-of-band direction finding, etc.[19,25,26,27] Also, there are usually some channels at the edge of the array that are passive and improve the sidelobes and RCS pattern.[8]

Figure 5.9 shows the comparison between a conventional mechanically scanned radar with the low-noise amplifier and a high-power traveling wave tube transmitter mounted off the gimbal versus a real-time adapted AESA with two different scan regimes for the same amount of input prime power. AESA performance falls off for large scan coverage because of the lower projected aperture area for a fixed mounting as shown in Figure 5.1. A mechanical scan has the same projected area in all directions and large scan angles marginally reduce radome losses, which results in slightly improved large angle performance. Nonetheless, AESA performance is usually superior inside

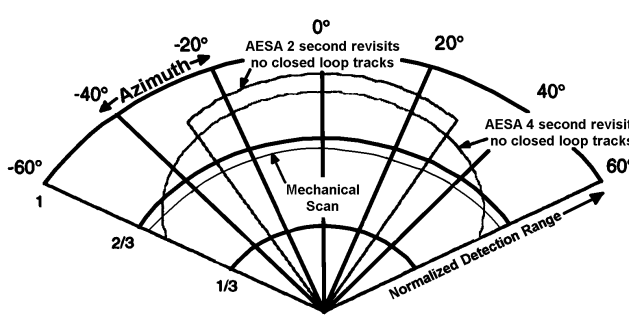

FIGURE 5.9 Example AESA management comparison (*adapted*[9])

a ±50° azimuth scan.[9,11,28] Usually, a fighter can't engage at long range outside this azimuth for kinematic reasons.

The performance differences depicted in Figure 5.9 are the result of three factors: the installed aperture can be 20% larger in net projected area at the aircraft in-flight horizontal due to elimination of gimbal swing space, 2:1 higher radiated power due to lower losses and better efficiency, and 60% lower losses before the low-noise amplifier. The other major advantage is that search volume can be changed dynamically to fit the instant tactical situation, as suggested in Figure 5.9.[28]

The feed network is mundane but critically important. In single tube transmitters, the feed is heavy because it must carry high power at low loss. AESA feeds use smaller coax, stripline, microstrip, or RF modulated light in fiber optics for transmit and receive RF, since less than 10 watts RF or optical is usually required. However, significant DC power is still required for RF feed distribution amplifiers because thousands must be driven. Cost, weight, and complexity is still an issue because multiple phase centers necessary for adaptive array performance require multiple manifolds. Usually, once a subarray is formed in the manifolds, it is digitized and multiplexed for adaptive signal processing.

Another important function is beam steering control (BSC). The BSC does array calibration, failed element compensation,[8,24] phase and amplitude setting for beam steering as well as space-time adaptive operation.[29–33] The BSC is usually realized with a combination of general purpose processing of the type found in a personal computer with very high speed incremental phase and amplitude calculation and T/R module interface hardware. Both scanning and adaptive operation require very low latency (i.e., the time between the sensed need and the first pulse at the target is usually 1 msec) beam control in a high-speed aircraft platform.

Lastly, the AESA requires a very significant power supply.[1] Power supplies have a history of being heavy, hot, and unreliable. Even the best systems still have overall power efficiencies (prime power in to RF out in space) in the 10–25% region in spite of years of development. The typical AESA requires low voltage and high current at the T/R channel. This forces large conductors in the absence of high power lightweight superconductors (not available at this writing). It also requires very low voltage drop rectifiers and regulators. Cooling is generally a significant performance burden. Usually, the power supplies are distributed to improve reliability and fault tolerance. Often, power converters are operated at switching frequencies up to several hundred megahertz to reduce the size of magnetics and filter components, and sometimes, the switching frequencies are synchronized to the radar master clock.

5.2 TYPICAL MISSIONS AND MODES

Air-to-Surface Mission Profile. The mode structure of any modern fighter aircraft arises from mission profiles.[7,9] One typical mission profile for an air-to-surface (A-S) strike is shown in Figure 5.10. The mission profile begins with a takeoff, continues through flight to a target, and ultimately returns to the starting point. Along the way, the aircraft uses a variety of modes to navigate, search and acquire targets, track targets, deliver weapons, assess battle damage, engage in countermeasures, and monitor and calibrate its performance. AESAs have demonstrated simultaneous multiple weapon deliveries.[22]

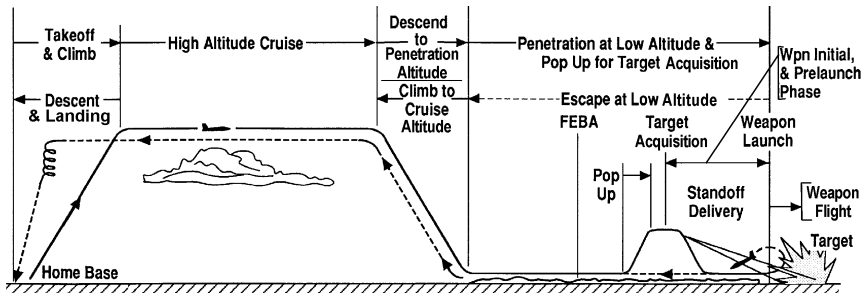

FIGURE 5.10 Typical air-to-surface mission profile[7,9]

Air-to-Surface Mode Suite. The mission naturally creates the need for an air-to-surface mode suite[7,9] for fighter radar, as shown in Figure 5.11. Each general category of operation contains modes primarily for that function, but modes will often be invoked during other parts of the mission. Within each mode shown in Figure 5.11, there is optimization for the particular combination of altitude, range to the target, antenna footprint on the Earth's surface, relative target and clutter doppler, dwell time available, predicted target statistical behavior, transmitted frequency, and desired resolution. Obviously, each mode must not compromise some required level of mission stealth.[34–37] A modern fighter is net-centric and exchanges substantial information with other systems. Both the fighter's wingman, support aircraft, and surface nodes may exchange complete data and tasking in real time to facilitate a mission. The fighter and its wingman will coordinate mode tasking so that during a high resolution ground map, which could take a minute to form, the wingman might be performing an air-to-air search and track to protect both of them.

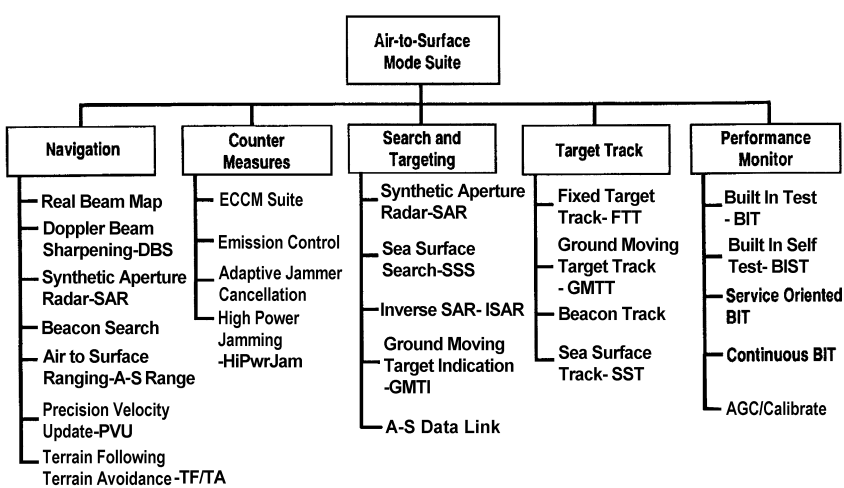

FIGURE 5.11 Fighter aircraft air-to-surface radar mode suite[7,9]

Some modes are used for several operational categories, such as real beam map (RBM), fixed target track (FTT), doppler beam sharpening (DBS), and synthetic aperture radar (SAR), used not only for navigation but also for acquisition and weapon delivery to fixed targets.[38–43] SAR may also be used to detect targets in earthworks or trenches covered with canvas and a small amount of dirt, which are invisible to EO or IR sensors. Similarly, air-to-surface ranging (A-S Range) and precision velocity update (PVU) may be used for weapon support to improve delivery accuracy as well as navigation.[7,9]

Terrain following and terrain avoidance (TF/TA) is used for navigation at very low altitudes or in mountainous terrain. Sea surface search (SSS), sea surface track (SST), and inverse synthetic aperture radar (ISAR), which will be described later in the chapter, are used primarily for the acquisition and recognition of ship targets. Ground moving target indication (GMTI) and ground moving target tracking (GMTT) are used primarily for the acquisition and recognition of surface vehicle targets but also for recognizing large movements of soldiers and materials in a battle-space. High power jamming (HiPwrJam) is a countermeasure available from AESAs due to their natural broadband, beam agile, high gain, and high power attributes. AESAs also allow long range air-to-surface data links (A-S Data Link) through the radar primarily for map imagery. Because there may be thousands of wavelengths and a gain of millions through a radar, automatic gain control and calibration (AGC/CAL) is usually required fairly often. Modes optimized for this function are invoked throughout a mission.

Waveform Variations by Mode. Although the specific waveform is hard to predict, typical waveform variations can be tabulated based on observed behavior of a number of existing A-S radar systems. Table 5.1 shows the range of parameters that can be observed as a function of radar mode. The parameter ranges listed are PRF, pulse width, duty cycle, pulse compression ratio, independent frequency looks, pulses per coherent processing interval (CPI), transmitted bandwidth, and total pulses in a Time-On-Target (T_{OT}).

Obviously, most radars do not contain all of this variation, but modes exist in many fighter aircraft, which represent a good fraction of the parameter range. Most fighter radars are frequency agile since they will be operated in close proximity to similar or identical systems. The frequency usually changes in a carefully controlled, completely coherent manner during a CPI.[8] This can be a weakness for certain kinds of jamming since the phase and frequency of the next pulse is predictable. Sometimes to counteract this weakness, the frequency sequence is pseudorandom from a predetermined set with known autocorrelation properties, for example, Frank, Costas, Viterbi, P codes.[16] A major difficulty with complex wideband frequency coding is that the phase shifters in a phase scanned array must be changed on an intra- or inter-pulse basis greatly complicating beam steering control and absolute T/R channel phase delay. Another challenge is minimizing power supply phase pulling when PRFs and pulsewidths vary over more than 100:1 range. MFAR systems not only have a wide variation in PRF and pulsewidth but also usually exhibit large instant and total bandwidth. Coupled with the large bandwidth is the requirement for long coherent integration times. This requirement naturally leads to extreme stability master oscillators and ultra low-noise synthesizers.[44]

Air-to-Air Mission Profile. Just as with an air-to-surface mission, the mode structure of a modern fighter aircraft air-to-air mission arises from its profile.[45] A typical mission profile for air-to-air (A-A) is shown in Figure 5.12. The mission profile

TABLE 5.1 Typical Waveform Parameters A-S Modes[7,9]

Radar Modes	PRF (kHz)	Pulse Width (μsec)	Duty Cycle (%)	Pulse Comp. Ratio	Freq. Looks	Pulses Per CPI	Transmitted Bandwidth (MHz)	Total Pulses in T_{OT}
Real-Beam Map	0.5–2	1–200	0.1–10	1–200	1–4	1–8	0.2–10	8–100
Doppler Beam Sharp.	1–4	1–60	0.3–25	13–256	1–4	20–800	5–25	20–1.6k
SAR	1–10	3–60	1–25	32–16384	1–4	70–20k	10–500	150–100k
A-S Range	1–8	0.1–10	0.1–10	1–256	4–8	1–8	1–50	5–100
PVU	2–100	1–25	0.01–25	1–16	4–32	20–1024	1–10	5–1000
TF/TA	2–20	0.1–10	0.05–5	1–32	16–64	1–8	3–15	20–60
Sea-Surface Search	0.5–2	1–200	0.1–10	1–20000	4–32	1–8	0.2–500	8–100
Inverse SAR	1–25	1–60	0.1–10	13–256	1–4	20–256	5–100	20–1000
GMTI	3–10	2–60	0.1–25	1–256	1–4	20–256	0.5–15	20–550
Fixed Target Track	2–20	0.1–10	0.1–10	1–256	4–8	1–8	1–50	20–1000
GMTT	2–16	2–60	0.1–25	1–256	1–4	20–256	0.5–15	20–1000
Sea-Surface Track	2–20	1–200	0.1–10	1–200	1–4	20–256	0.2–10	20–1000
HiPwr Jam	50–300	3–10	10–50	13–512	1–8	1–8	1–100	200–2k
Cal/A.G.C. A-S Data Link	0.5–20 8–300	0.1–200 0.8–20	0.01–50 1–100	1–16384 13–32768	1–8 1–75	8–64 100–500	0.2–500 0.5–250	8–64 1.3k–80k

begins with an airfield or carrier takeoff, continues through flight penetrating into an enemy battle-space, searches for air targets to attack, and ultimately returns to the starting point. Along the way, the aircraft uses a variety of modes to navigate; exchange data with command, control, communications, intelligence, surveillance,

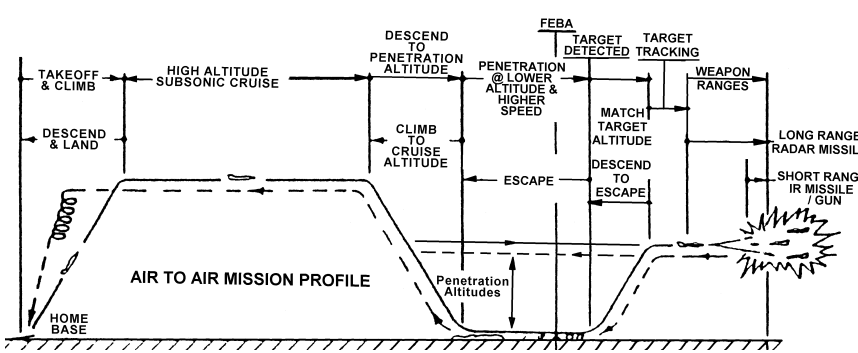

FIGURE 5.12 Typical A-A mission profile[45]

reconnaissance (C3ISR) assets; search and acquire airborne targets; track and separate benign targets from threats; deliver weapons; escape and engage in countermeasures; monitor and calibrate its performance, and return to base.

Air-to-Air Mode Suite. Similarly, the A-A mission naturally creates the need for a corresponding mode suite for the radar, as shown in Figure 5.13.[46,47] At the radar sensor and air-to-air mode software level, there is adaptive task prioritization to insure that the highest processor prioritized, pilot-selected threat is serviced first. Passive modes are interleaved with active operation to improve survivability and passive tracking and ID. Each mode shown in Figure 5.13 is optimized in real time for the particular combination of altitude, range to the target, density of target threats, antenna footprint on the Earth's surface, relative target and clutter doppler, dwell time available, predicted target statistical behavior, transmitted frequency, and desired resolution.[9,11]

The mode category "autonomous and cued search" contains the modes most commonly associated with fighter radars. There are usually two range-gated high pulse repetition frequency (HPRF) modes: velocity search (VS) primarily dedicated to longest range detection and range while search (RWS), which uses some form of FM ranging to estimate target range. There is a medium PRF (MPRF) mode, which provides all aspect velocity-range search (VRS) at the expense of poorer long-range performance. In addition, there are two passive modes: passive search and ranging, in which the radar detects and estimates range and angle to an emitter or bistatically (wingman or support aircraft) illuminated target and ESM shared aperture in which the RF and processor complex detects, estimates waveform parameters, and records them for future use. Passive search may be combined with cued burst ranging to better estimate emitter location. Extended volume search is a mode used with cueing from another on- or off-board sensor in what normally would be an unfavorable geometry.[85]

Many modes and functions are shared in common with A-S, especially countermeasures and performance monitoring. Extremely important in both modes is implementation of emissions control to minimize the ability of the adversary to detect, track, and attack using the radar emission.[16] Without care, these emissions can easily serve as a strong guidance signal for a hostile antiradiation missile (ARM).[50,51] Antenna apertures that have multiple independent phase centers can perform both adaptive clutter cancellation as well as jammer cancellation with suitable hardware and software.[14,27,29–33]

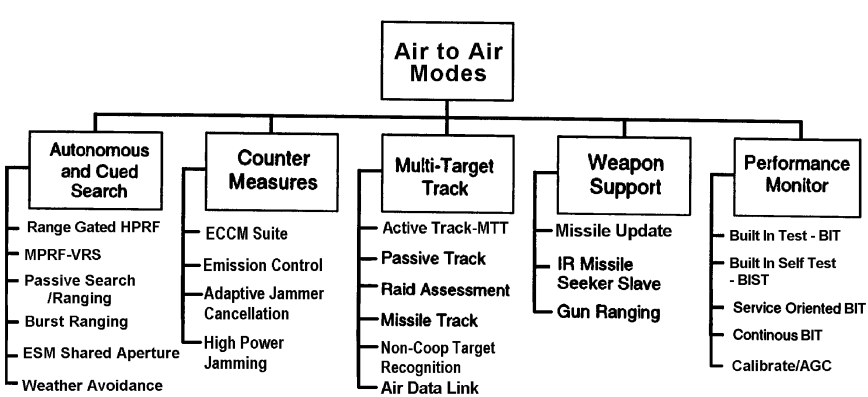

FIGURE 5.13 A-A mode suite[9]

The subsuite of multi-target track (MTT) contains conventional track while scan (TWS), passive tracking of emitters or echoes from bistatic illumination, missile tracking with or without a missile datalink or beacon, and several modes to recognize target number and type: raid assessment and noncooperative target recognition (usually incorrectly called *target identification*). The fighter and wingman will coordinate modes through the net so that both have situational awareness during the long time span required to provide target recognition.

Another important fighter category is weapon support. Missile update is the measurement of missile and target position, velocity and acceleration to allow statistically independent measurements for transfer alignment, as well as missile state-of-health. Missile update provides the latest target information and future dynamics prediction by data link. IR missile slaving co-aligns radar and seeker. Since gun effective ranges are very short, gun ranging causes the radar to sense the gun field of fire, predicts angle rate, and measures range to a target for tentative gunfire.[9] It may also track gun rounds during fire.

There are thousands of electrical degrees of phase between free space and the A/D converters. The combination of temperature, time, and manufacturing tolerances gives rise to the need for self calibration, test, fault detection, failure diagnosis, and needed corrections, which are performed by a subsuite of performance monitor software.

Timing Structure. The significance of the remaining parameters in Tables 5.1 and 5.2 can best be illustrated with a timing structure typical of fighter radars.[7,8,9] Figure 5.14 shows a modern radar timing structure in a sequence of progressively expanded timelines. The first row of Figure 5.14 shows a typical scan cycle covering the required volume of interest for a specific mode. The time span for a full scan cycle might be 1 to 5 seconds. Inside the total scan cycle time, there may be several bars of a scanned region of space with a time span of a few tenths of a second. A bar is a scan segment along a single angular trajectory, as shown in Figure 5.20, later in the chapter.

TABLE 5.2 Typical Waveform Parameters A-A Modes[9]

Radar Modes	PRF (kHz)	Pulse Width (μsec)	Duty Ratio (%)	Pulse Comp. Ratio	Freq. Looks	Pulses Per CPI	Instant Band-Width (MHz)	Total Pulses in T_{OT}
Range-Gated High PRF	100–300	1–3	10–30	1–13	1–4	500–2000	0.3–10	1500–6000
Medium PRF	6–20	1–20	1–25	5–256	1–4	30–256	1–10	250–2000
Burst Ranging	3–20	2–60	0.1–25	1–256	1–4	20–256	0.5–15	20–550
Active Track	8–300	0.1–20	0.1–25	1–256	4–8	1–64	1–50	20–1000
Raid Assessment	2–16	2–60	0.1–25	1–256	1–4	20–256	0.5–15	20–1000
Non Coop. Target Rec.	2–20	1–200	0.1–10	1–16384	1–4	20–256	0.2–100	20–1000
HiPwr Jam	50–300	3–10	10–50	13–512	1–8	1–8	1–100	200–2k
Cal/AGC	2–300	0.1–60	0.01–50	1–16384	1–8	8–64	0.2–500	8–64
Air Data Link	10–300	1–20	1–33	1–16	1	100–500	0.1–1	100–500
Gun Ranging	10–20	0.1–0.5	0.1–1	1–5	1–4	4–32	1–10	4–128
Weather Avoidance	0.5–5	1–50	1–10	1–13	1–2	1–8	0.1–1	1–16

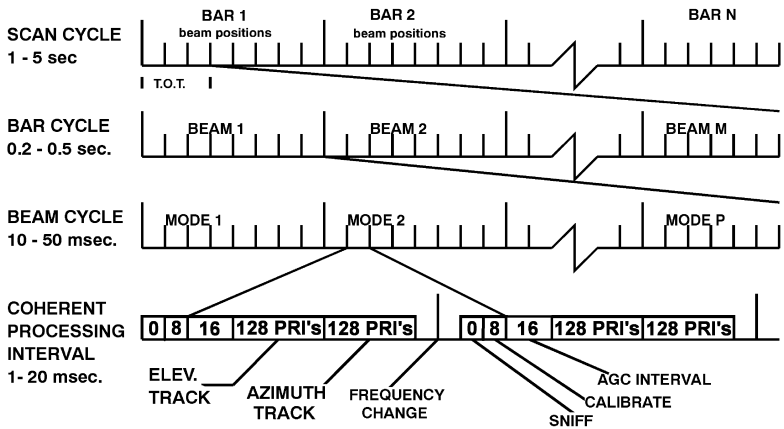

FIGURE 5.14 Typical MFAR timing sequences[7,8,9] (*Courtesy SciTech Publishing*)

Each bar consists of multiple beam positions of a few tens of milliseconds each, which are computed on the fly to optimally cover the selected volume. Each beam cycle, in turn, may contain one or more radar modes or submodes, such as those contained in Tables 5.1 or 5.2 and depicted in the lowest line of Figure 5.6. The modes may not be invoked each time depending on the geometry between the aircraft and the intended target set.

The mode time is broken up into coherent processing intervals (CPI's). A coherent processing interval is segmented, as shown in the bottom row of Figure 5.14. The particular example shown is tracking that might be used in FTT, GMTT, PVU, or A-G Ranging, as shown previously in Figure 5.10, and later in Figures 5.32 and 5.38. It consists of a frequency change; settling time; passive receiving to be sure the band isn't jammed; calibrate that doesn't intentionally radiate but often there is some RF leakage radiated; an automatic gain control (AGC) interval in which a number of pulses are transmitted to set the receiver gain; and finally two intervals in which range, doppler, and angle discriminants are formed. These CPIs often but not always have constant power, frequency sequence, PRF sequence, pulsewidth, pulse compression, and bandwidth.[7,8,9]

5.3 A-A MODE DESCRIPTIONS & WAVEFORMS

Air-to-Air Search, Acquisition and Track— Medium PRF. It may be instructive to examine how several modes are generated and processed to understand why the waveforms must be the way they are. Medium PRF trades long-range detection performance (see Figure 5.21, later in the chapter) for all aspect target detection.[28,52,53] Often high and medium PRF waveforms are interleaved on alternate scans (see Figure 5.20) to improve total performance.[28,54,55] After 30 years of searching for an optimum set, most modern medium PRF modes have devolved to a range of PRFs between 8 and 20 kHz in a detection set of 8 for the time on target.[44,56–61] These PRFs are chosen to minimize range and velocity blind zones while simultaneously allowing unambiguous resolution of target range and doppler returns in a sparse target space.[62,63,64] Range blind zones are those ranges in which a target is eclipsed by the transmitted pulse. Velocity or doppler blind zones are those velocities or dopplers that are excluded due to the

main-beam clutter and ground moving target filter rejection notch. Target detection requires detections in at least 3 of the 8 PRFs with all PRFs clear at maximum range. The PRF selection criteria usually requires that the PRF set is 96% clear—in other words, at least a specified number (typically 3) of PRFs must have an above threshold return echo for the minimum specified target for the full specified range-doppler coverage.

A typical processing block diagram is given in Figure 5.15. Each PRF processing interval is different, but they average out to an optimum, as shown later in Figure 5.17. Both main and guard channel processing is required to reject false targets.[25] Some STAP processing may have been performed before this process, but traditional sidelobe and main-beam clutter is less of a limit than ground moving targets, which have very large cross sections and exo-dopplers (i.e., doppler far enough out of main-beam clutter that detection is not limited by the clutter return). MPRF usually has a small amount of pulse compression (1:1 to 169:1), which still may require doppler compensation.[65] Main and guard channels are processed in the same way. Obviously, the two spectra are quite different and separate false alarm and noise ensemble estimates are made. This leads to separate threshold settings. Multiple channels are used to estimate interference and select ECCM strategy. Main channel detections are examined for GMTs and centroided in range and doppler (because a return in range or doppler may straddle multiple bins, the centroid of those returns in multiple bins must be estimated from the amplitude in each bin and the number of bins straddled). The guard channel is detected and the thresholded results are used to gate the main channel results for the final hit-miss count. Genuine targets are resolved in range and doppler, presented to a display and used for TWS correlation and tracking.[8]

False alarms are a critical issue in most radar modes. These are usually suppressed for thermal noise by constant false alarm rate thresholding, coincidence detection, and post-detection integration with frequency agility. Clutter false alarms are suppressed by adaptive aperture tapering, low-noise front-end hardware, wide dynamic range A/Ds, clutter rejection filtering (including STAP), pulse compression sidelobe suppression, doppler filter sidelobe control, guard channel processing, radome reflection lobe compensation, angle ratio tests (see Figure 5.37 and the "fringe region" for an example angle-ratio- test), and adaptive PRF selection.

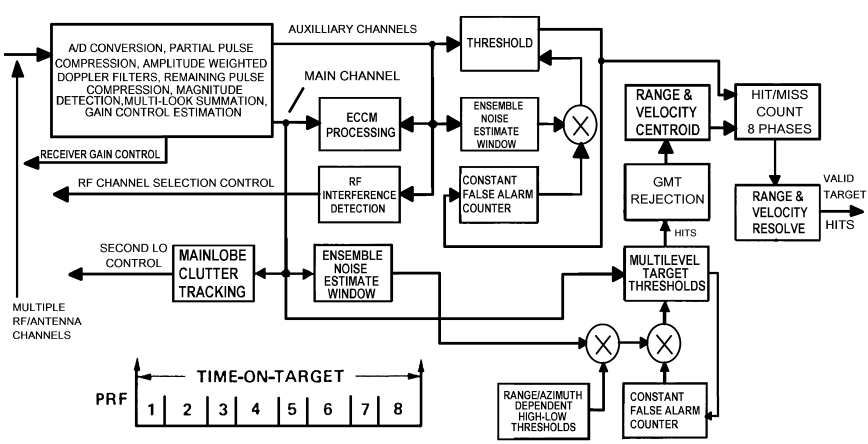

FIGURE 5.15 Typical MPRF processing (*adapted*[8]*; courtesy SciTech Publishing*)

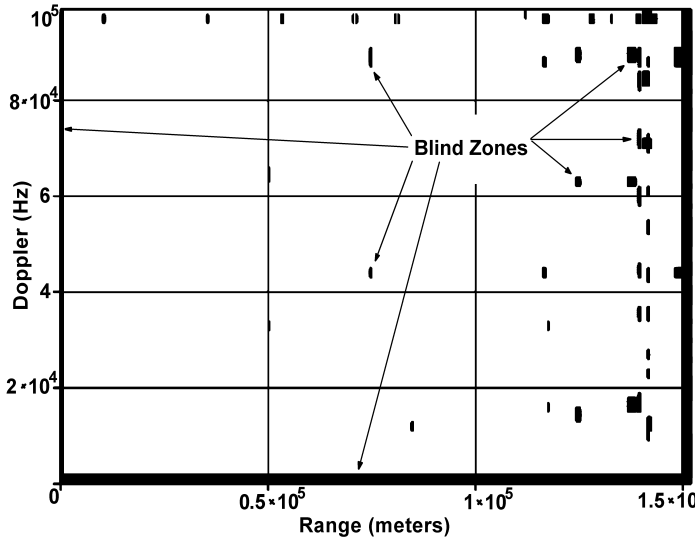

FIGURE 5.16 Medium PRF range-velocity blind zones

MPRF-Typical Range-Doppler Blind Map. For example, a typical MPRF set for X band with range-doppler coverage of 150 km–100 kHz is shown in Figure 5.16. This set is for a 3° antenna beamwidth, ownship (i.e., the radar carrying fighter) velocity of 300 m/s, and an angle off the velocity vector of 30°. The PRF set is 8.88, 10.85, 12.04, 12.82, 14.11, 14.80, 15.98, and 16.77 kHz. Historically, a PRF set was calculated during design and remained fixed during deployment. Modern multifunctional radar computing is so robust that PRF sets can be selected in real time based on situation geometry and look angle. The set, which generated Figure 5.16, on the average is clear on 5.6 out of 8 PRFs for a single target. Except for two small doppler regions, all the PRFs are clear at maximum range, which provides maximum detection and minimum loss at the design range. For some pulse compression waveforms, the eclipsing loss is almost linear and partial overlap still allows shorter-range detection. Eclipsing loss is that diminishment of received power when the receiver is off during the transmitted pulse. It is often the largest single loss in high duty ratio waveforms. The bad news is that the average detection power loss is slightly over 3 dB (see Figure 5.21).

MPRF Selection Algorithms. Obviously, selecting PRFs in real time requires several rules to get close to a final set. This is followed by small iterations to pick the optimum set. For medium PRF, both range and velocity blind zones are important.[52,65] First, the software must pick a central PRF about which all the other PRFs are deviations to fill out the desired visibility criteria. Second, the PRF set should all be clear at the maximum design range so that detection losses are at a minimum.

Figure 5.17 shows one example criteria for selecting the central PRF, i.e., the highest probability of visibility (P_V).[45] In the example, the product (P_V) of the range (P_R) and doppler (P_D) target visibility probabilities for a single PRF peaks at approximately 0.47 and thus the other PRFs must fill in to reach 96% clear or higher. There are several

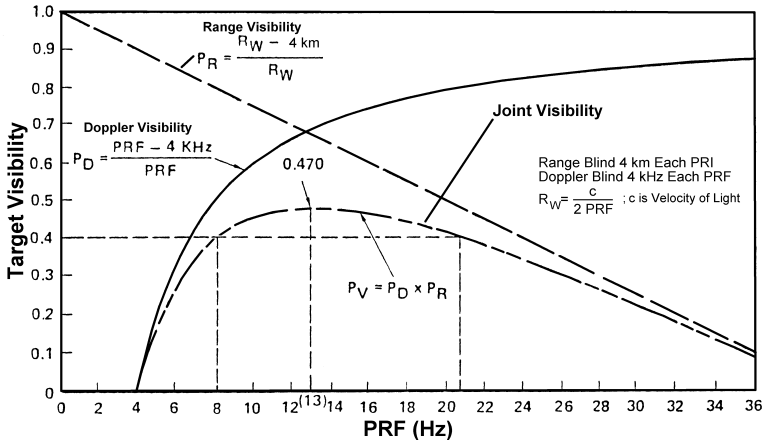

FIGURE 5.17 Medium-PRF central PRF selection example[45]

other factors to be considered: doppler and range blind zones and eclipsing and sidelobe clutter. Even with STAP, sidelobe clutter is a major limitation.[67,68,93] Both sidelobe and main-beam clutter can be minimized by narrow doppler and/or range bins (i.e., resolution cells), which imply longer dwell times and higher transmit bandwidth.

One example method for selecting a set of PRFs for MPRF is given in Eq. 5.1. The basic idea is to find a time interval, T_A, representing the desired maximum clear range, and then to choose a set of PRIs in which all will be clear at maximum range. This can be achieved by dividing T_A by an integer, typically 9 to 17. This set will generally not provide 96% clear over the range-doppler space. The even divisor PRIs can be perturbed iteratively by a small amount to achieve the desired visibility. The normalized target signal-to-noise ratio, TP, varies dramatically with straddle and eclipsing losses (for example, see Figure 5.18). The function to be optimized is a thresholded version of $TP_{k \text{ or } j}$.

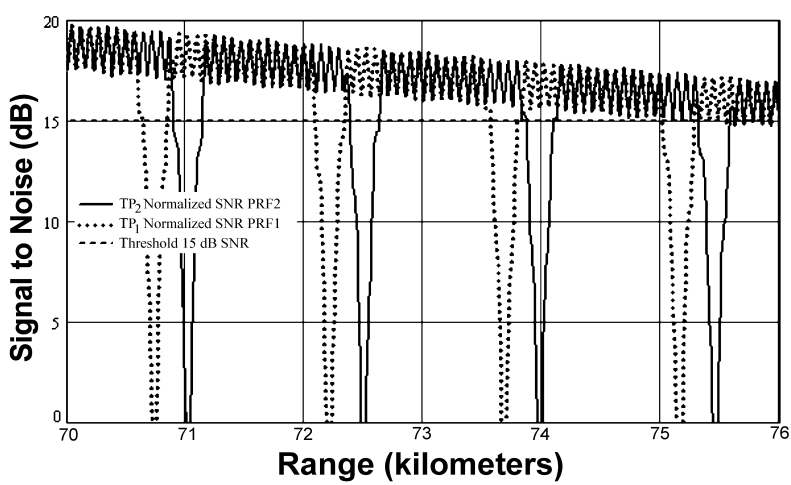

FIGURE 5.18 Example RGHPRF eclipsing and straddle near maximum range

For example, the threshold scheme might be 15 dB SNR per PRI and 3 out of 8 for all PRIs. Often multiple and different thresholds are used for each CPI and PRI. Lower thresholds are allowable for higher numbers of total hits.[28] It should be noted that eclipsing and straddling, and so on, have much less effect at closer ranges where there is usually more than enough SNR. Another serendipitous effect of this selection technique is that as an individual PRI range clear region gets smaller, the doppler clear region gets larger, filling-in the blind zones in both dimensions.

$$T_A = 2 \times \left(\frac{R_c}{c} + \tau_p \right), PRI_k = \frac{T_A}{C_1 + 2 \times k}, PRI_j = \frac{T_A}{C_2 + 2 \times j + \delta_j}$$
$$TP_{k \text{ or } j}(f,r) = \frac{C_3}{r^4} V_{\text{blind}}[\text{mod}(f, 1/PRI_{k \text{ or } j})] \times R_{\text{blind}}[\text{mod}(r, PRI_{k \text{ or } j})] \quad (5.1)$$

where: R_c is maximum design clear range
c is the velocity of light $2.9979 \cdot 10^8$ m/s
τ_p is transmitted pulse width, k and j are indices e.g. 0…4
C_1 is an odd integer e.g. 9, C_2 is an even integer e.g. 12
δ_j is a small perturbation e.g. 0.1…0.3 yielding visibility > 96%
V_{blind} is a function of f describing eclipsing and straddling
R_{blind} is a function of r describing eclipsing and straddling
C_3 is a constant representing the remainder of the range equation
f is frequency, r is range, mod is modulo the first variable by the second

Range-Gated High PRF. Range-gated high PRF (RGHPRF) performance is dramatically better for detection of higher speed closing targets.[44,54,55,70] (Range gates are often smaller than range resolution cells or bins). RGHPRF produces the longest detection range against closing low cross section targets.[71] Ultra-low noise frequency references are required to improve subclutter visibility on low RCS targets even using STAP. Range gating dramatically improves sidelobe clutter rejection, which allows operation at lower ownship altitudes. Principal limitations of RGHPRF closing target detection performance are eclipsing (a radar return when the receiver is off during the transmitted pulse) and range gate straddle losses (the range gate sampling time misses the peak of the radar return).[15] Figure 5.18 shows TP_i with eclipsing and straddle losses near maximum range for a high performance RGHPRF. This mode is optimized for low cross section targets out to just beyond 75 km maximum range. The particular example has overlapping range gates to minimize straddle loss and two PRFs to allow at least one clear PRF near maximum range. The PRFs are 101.7 kHz and 101.3 kHz. Duty ratio is 10% with 15 dB required detection SNR. Averaged over all possible target positions and closing dopplers, the losses for this mode are a surprisingly small 0.4 dB.

The range-doppler blind zones plot is shown in Figure 5.19 corresponding to the Figure 5.18 waveform. Compared to the medium PRF plot shown in Figure 5.16, the clear region (and corresponding losses) is dramatically better. Unfortunately, range is very ambiguous. Normally, a RGHPRF range-while-search (RWS) mode is interleaved with the highest performance velocity-search (VS) mode to range on previously detected targets.

Often, RWS is RGHPRF with three phases in which a constant frequency and two chirp (linear FM) frequencies (triangular up-down or up-steeper up) are used to resolve range and doppler in a sparse target space. At low altitudes, sidelobe clutter, even with STAP processing, limits performance for all targets but especially opening targets.

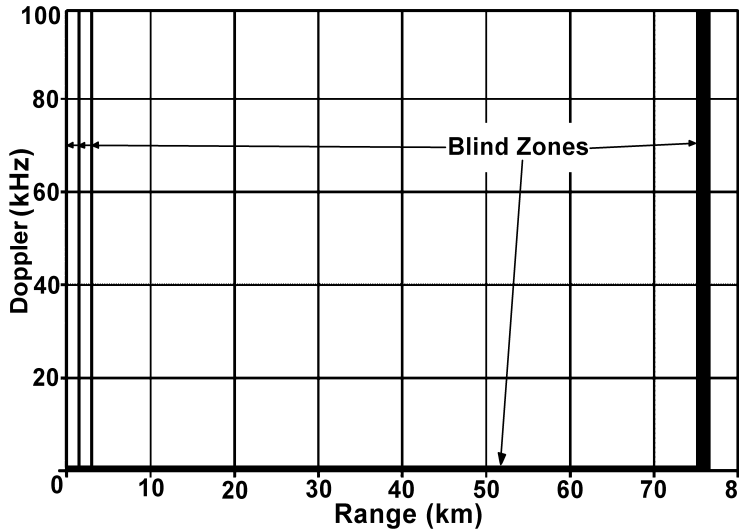

FIGURE 5.19 RGHPRF range-velocity blind zones, corresponding to Figure 5.18 waveforms

This limitation leads to the need for another mode interleaved with RGHPRF. Fortunately, the timeline for opening targets is much longer (net speed is less) and the engagement range is much shorter (weapon closure rates are too slow).

Often in general search, MPRF-VRS (medium PRF velocity-range search) is interleaved with HPRF VS and RWS, as shown in Figure 5.20, to provide all aspect detection. Unfortunately, both RWS and VRS have poorer maximum detection range. RGHPRF can provide all aspect detection but tail performance is dramatically poorer due to sidelobe clutter. Even with STAP, which significantly improves sidelobe clutter rejection, low altitude tail aspect detection for RGHPRF is poorer.[44,45,55]

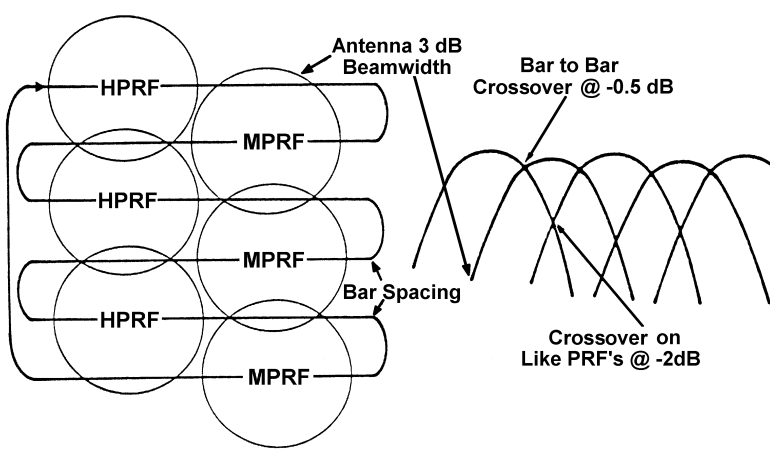

FIGURE 5.20 High and medium PRF interleave for all aspect detection[45]

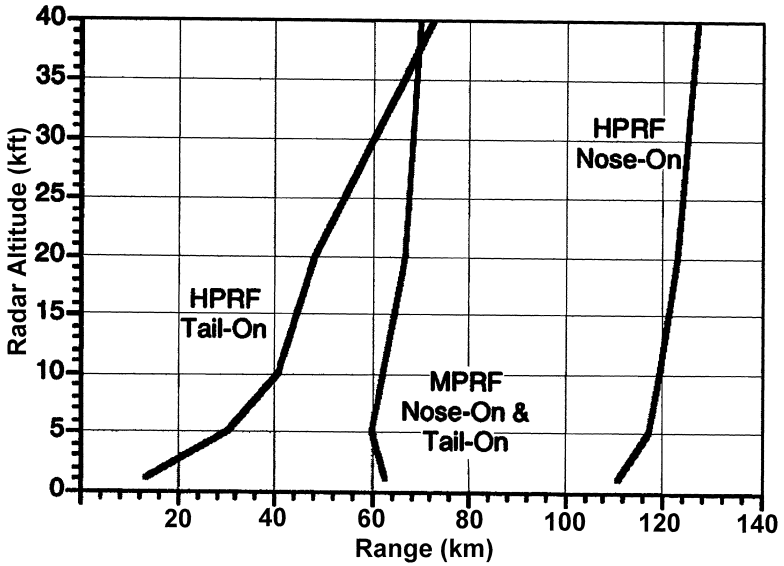

FIGURE 5.21 Comparison of high and medium PRF[9]

An example comparison of HPRF and MPRF as a function of altitude for a given maximum transmitter power, power-aperture product, and typical antenna and radome integrated sidelobe ratio is shown in Figure 5.21. At high altitude and nose-on, there is more than an 11 dB difference caused by blind zones, straddle, folded clutter, processing, and thresholding losses.[9,11,28]

RGHPRF Selection Algorithms. First, as in the MPRF case, all PRFs should be clear at the maximum design range. Second, all PRFs should be clear to the maximum doppler of interest. One possible selection criteria is given in Eq. 5.2. Although the details are quite different, the basic philosophy in PRF selection is to optimize long-range clear regions.

$$T_A = \frac{2 \times R_c}{c} + \tau_p \text{ and } PRI_A = \frac{0.25 \times \lambda}{V_a + V_t} \text{ and } I = \text{ceil}\left[\frac{T_A}{PRI_A}\right]$$

$$\text{then } PRI_1 = \frac{T_A}{I} \text{ and } PRI_2 = PRI_1 \times \left[\frac{c \times \tau_p}{R_c} + 1\right] \tag{5.2}$$

where: R_c is maximum design clear range,
c is the velocity of light 2.9979×10^8 m/s,
τ_p is transmitted pulse width, λ is transmitted wavelength,
ceil is the next integer above the value of the variable,
V_a and V_t are the maximum velocities of interest for aircraft and target respectively.

Noncooperative Air Target Recognition[72] MFAR target recognition (TID) recognizes target type but not unique identification. There are cooperative target

identification methods such as JTIDS, IFF, and RF tagging that can be unique. TID depends on detecting features of the radar signature in fusion with emissions and other sensors. The five most common TID signatures are monopulse extent (similar to the example shown in Figure 5.25), resonances, high resolution range (HRR) profiles, doppler spread, stepped frequency waveform modulation or multifrequency (SFWM/MFR), which can be transformed into a range profile, and inverse synthetic aperture radar (ISAR).[16,45] Monopulse extent allows estimation of length and width as well as separation of closely spaced aircraft. A high range resolution profile also allows the separation of targets flying in close formation as well as the separation of a missile from a target. A high range resolution profile on a single target can allow recognition, assuming the target attitude is known or has been guessed. Length, width, and location of major scattering features can be projected into a range profile if the attitude is known. The number of types of major civilian and military aircraft and ships is at most a few thousand, easily storable in memory. Unfortunately, recognition is limited to broad categories rather than MIG-29M2 versus MIG-29S (even though there are significant differences that air show visitors can easily see[89]).

The basic notion of doppler, resonances, stepped (SFWM), and multifrequency (MFR) signatures is modulation either by reflections from moving parts, e.g., engine compressor, turbine, rotor, or propeller blades, or by interactions from scatterers along the aircraft or vehicle, e.g., fuselage, wing, antennas, or stores. SFWM/MFR signatures are closely related to high range resolution signatures (a Fourier transform easily converts one to the other), and they suffer the same attitude estimation limitations. The principal advantage to MFR is that many deployed radars have multiple channels and switching between them on a single target is relatively easy. A simplified version of the recognition process is summarized in Figure 5.22.

Doppler signatures require high doppler resolution, which is usually easily achieved and limited only by dwell time. The individual scatterers, which give rise to doppler spread, are small and so recognition is usually limited to a fraction (1/2 typical) of maximum range. Jet engine modulation (JEM), a subset of doppler signatures, is an excellent target recognition method. Even aircraft, which use the same engine type, often have variations in the engine application, such as the number of compressor blades or number of engines, which allows unique type recognition. The real picture of JEM is not so clean because of multiple on-aircraft bounces, straddling, and speed variations, but centroiding of each line improves the signature estimate. The last method of TID, ISAR, will be dealt with in another section. ISAR works well on both aircraft and ships. A typical tail hemisphere air-to-air ISAR is shown in Figure 5.23.

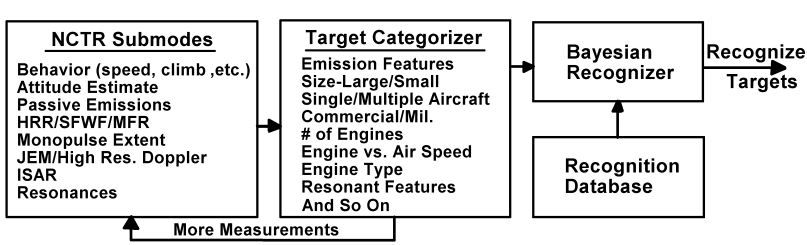

FIGURE 5.22 Noncooperative target recognition submodes[45]

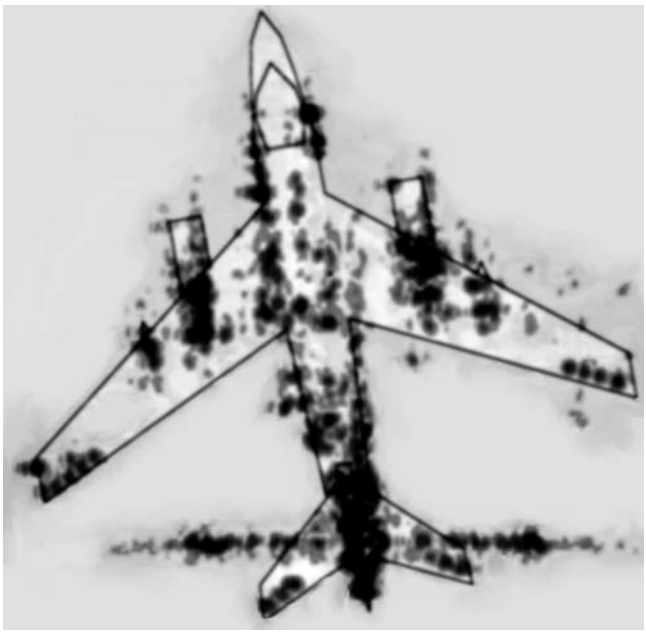

FIGURE 5.23 A-A ISAR example TA-3B[45]

The fusion of the recognition of each of the signatures above provides excellent noncooperative recognition.

Weather Avoidance. Many aircraft have separate weather radars. Weather avoidance is normally incorporated into modern fighter radars. The normal operating frequency for a fighter radar has not been considered optimum for weather detection and avoidance[15]—primarily due to lack of penetration depth into a storm and reduced operating range. However, with complex atmospheric attenuation compensation and doppler methods, weather can be detected well enough to allow warning and avoidance of storms. The principal challenge is compensating for backscatter from the leading edge of a storm and adjusting for attenuation to see far enough into a storm to evaluate its severity. The backscatter from each cell is measured, the power remaining is calculated, the attenuation in the next cell is estimated, and then the backscatter in the next cell is measured, and so on. When the power in the cells drops to the noise level, those cells behind it are declared blind. Since penetration range into a storm is not great, the MFAR weather mode usually has provisions to mark the last visible or reliable range on the weather display. This is so the pilot does not fly into a dark area believing there is no weather.

Air Data Links. The MFAR is part of a network of sensors and information sources (C3ISR net) sometimes called the *Global Information Grid (GIG)*. A major use of radar and aircraft data links is to provide total situational awareness.[21] By using on-board and off-board sensor fusion, a total air and ground picture can be presented in the cockpit. This picture can be a combination of data from

other radar sensors (wingman or support aircraft) on similar platforms to reports by observers with binoculars. Because the modern fighter is net-centric, using everything available on- and off-board the aircraft, net-centric operation requires dramatically higher levels of data exchange and fusion of data for presentation to the operator. Radar modes can be scheduled between multiple aircraft in real time through the data links.

The two main uses for data links associated with high performance aircraft are high bandwidth imagery transmission from a weapon or sensor platform to a second platform or ground station and low bandwidth transmission of context, targeting data, guidance, and housekeeping commands.[74–79] The largest quantity of data links are associated with weapons. The waveform selected to transmit this and other data must not compromise the signature of the platform at either end of the link.[8,34–37]

There are numerous data links on fighters. Table 5.3 shows air data links that might be on a fighter platform. In spite of this fact, the radar or part of its aperture is often used for a data link, especially to missiles on the fly and in response to peacetime air traffic control interrogations. Pulse amplitude (including on-off), pulse position, phase shift, and frequency shift modulation are commonly used. Links may be unidirectional or bidirectional. Some missiles require semi-active illumination as well as reference signals and midcourse command data derived from missile and target tracking. The data to and from the missile is often an encrypted phase-code in or near the radar operating band. In some cases, the frequency channel is randomly selected at the factory and hardwired into the missile. Frequency channels are typically selected or communicated to the radar immediately before launch. If the data link frequency is well below the radar band, usually a small number of radiators at that lower frequency are imbedded in the radar aperture. If the frequency is close enough to the radar band, the radar aperture or a segment of the aperture is used.

Radar Aperture Datalinking.[81] Historically, datalink functions embedded in MFARs have been used for the midcourse guidance of missiles. An emerging application is the use of the radar aperture as a high power, high gain primary datalink antenna,

TABLE 5.3 Air Data Links[80]

Link	Freq Band	Data Rate (kb/s)	ECCM
ARC-164	UHF	1.8	High
ARC-126	UHF	1.8	High
ARC-201	VHF	8	Moderate
ARC-210	VHF/UHF	8	Moderate–High
TADIL	UHF-L	1.8–56.6	Moderate–High
JTIDS	L	28.8–56.6	Moderate
JTIDS LET	L	383.6–1,180.8	Moderate
JTRS	VHF-X	1.8–1,544	Moderate–High
TADIXS	UHF	9.6	Moderate
MFAR	X-Ku	2–105	Moderate–High
Milstar	UHF, Ku - Ka	4.8–1,544	High
TCDL	X - Ku	1,000–256,000	Moderate

where datalink transmission and reception are interleaved with other modes. The principal limitation of most general-purpose datalink equipment is the low power-aperture performance associated with omnidirectional, often shared, antenna apertures and limited power levels. This constrains achievable data transfer rates, regardless of channel bandwidth. An associated problem is vulnerability to intercept and jamming inherent in widebeam apertures. An X or Ku band MFAR can emit power levels in the multi-kilowatt range with main-beam beamwidths of a few degrees, affording high data rates and significant resistance to jamming and intercept. Transmit data rates of over 500 Mbps, and receive data rates of up to 1 Gbps have been demonstrated using a production AESA and a modified Common Data Link (CDL) waveform.[82] Modeling using representative MFAR parameters indicates that performance bounds are at several Gbps throughput over distances in excess of 400 nautical miles, subject to MFAR performance, platform altitude, tropospheric conditions, and forward scattering effects.[81]

Implementation requires accurate antenna pointing, since there is relative motion with respect to the other end of the link. One technique involves the use of an out-of-band datalink channel, e.g., JTIDS, to carry GPS position updates.[83] Doppler shifting due to link geometry dynamics must be actively compensated. A related issue is synchronization in time to allocate transmission and reception windows and to synchronize timebases. When existing waveforms must be used, this can present challenges. Existing aperture scheduling algorithms can then allocate time for transmission or reception.[81]

To achieve very high throughputs, phase linearity in transmit and receive paths is critical since data transmission waveforms rely on modulation that is every bit as complex as many radar modes. This can also impact choice of taper function because angular variations in phase across the main-beam wavefront may incur performance penalties. Where the MFAR is phase steered, aperture fill and sidelobe steering effects constrain usable aperture bandwidth similar to SAR limitations. The latter is because the element phase angles required to point the main beam are not the same as those for the outer sidelobes of the modulation used.[81]

Low bandwidth data links can use all the radar bandwidth to improve encryption and signal-to-jam ratios. However, the data link on a weapon is traveling to the target, which will inevitably attempt to protect itself. When the weapon is near the target, the signal-to-jam ratio can be very unfavorable. Antenna jammer nulling is usually required since transmitting more power to burn through may not be possible. Clearly, the data from and to a weapon must also be sufficiently encrypted to prevent take-over of the weapon in flight.[8]

Time synchronized with a radar transmission on a different set of beams and/or frequencies, messages are sent to one or more missiles on the fly to the targets. Obviously, all the random frequency diversity, spread spectrum, and encryption necessary for robust communication should be incorporated into the message.[78] Each missile may answer back at a known but randomized offset frequency and time with image or housekeeping data. Again a waveform as robust as possible is used, but since the baseband data and link geometry may be quite different, the data compression, diversity, and encryption may be different.

The missile datalink waveform usually must be stealthy and greatly attenuated in the direction of the target since one countermeasures strategy is a deception repeater jammer at the target. High accuracy time and frequency synchronization, including range opening and doppler effects between both ends of the link can dramatically reduce the effectiveness of jamming by narrowing the susceptibility window. Time and frequency synchronization also minimizes acquisition or reacquisition time.

An aircraft using a data link is moving with respect to the other end of the link, so the link geometry is continually changing in time, frequency, aspect, and attitude. The signal processor will generate waveforms for transmission by the seeker or data link. It will also measure target range, angle, doppler, and so on, and provide those to the other platform. The MFAR signal processor sends motion sensing and navigation estimates to correct measurements; to track, encode, and decode datalink messages; and to perform jammer nulling.

Beacon Rendezvous and Station Keeping. Most modern military aircraft depend on in-flight refueling for many missions. This requires rendezvous with tanker aircraft during all weather conditions as well as station keeping until aircraft currently in line for refueling depart. This may involve detecting a coded beacon on the tanker, skin tracking tankers and other aircraft at close range. Station keeping ranges can be between 30 and 1000s of meters. Special short-range radar modes are usually used for this purpose. Low power, short pulse or FM-CW waveforms are often used. One meter accuracy and 30 meter minimum range is usually required for blind tanking.

High Power-Aperture Jamming. The basic notion behind MFAR high power-aperture jamming is suggested in Figure 5.24.[9,11,71,84]

A threat emitter, whether surface or airborne, is first detected and recognized by the spherical coverage radar warning receiver (RWR) function (possibly just an application overlay on the RF and processing infrastructure shown in Figure 5.4). If the intercept is inside the radar field of view (FOV), fine angle-of-arrival (AOA) and possibly burst ranging are performed with the primary radar aperture, as shown in the top portion of Figure 5.24. High-gain electronic support measures (ESM) are then performed and recorded on the emitter main beam or sidelobes using the nose aperture. If it is determined from an on-board threat table, current rules of engagement, or mission plan, high power density jamming based on the corresponding on-board techniques table may be initiated using the high-gain nose aperture.[84]

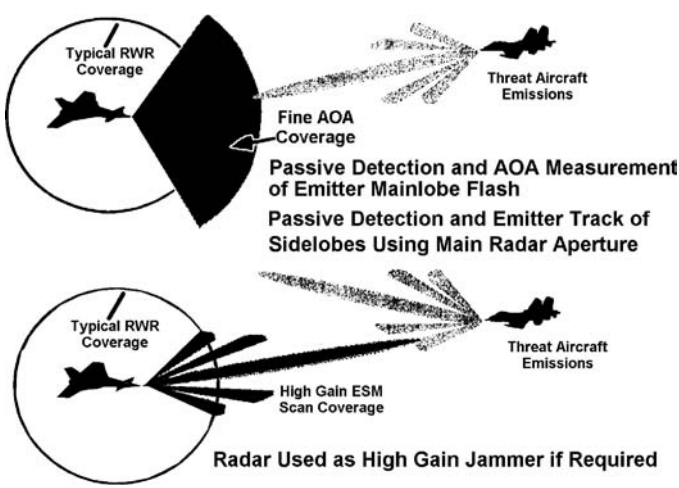

FIGURE 5.24 MFAR ECM example[9]

Because the adversary radar may also be a MFAR, threat tables will be required to categorize them by their apparent statistical nature. Old style matching by PRF, pulsewidth, and pulse train envelope won't work very well because waveforms vary so much. The typical nose aperture radar–based effective radiated peak power (ERPP) can easily exceed 75 dBW, which is normally more than enough to play hob with threat radars.[39,85] For example, assuming a 10 GHz in-band signal, –3 dBi threat sidelobe, and –110 dBW threat sensitivity, a jamming pulse 60 dB above minimum sensitivity can be generated at 20 km. Obviously, in the near sidelobes or main beam, the range for a 60 dB pulse will be much greater.[84]

5.4 A-S MODE DESCRIPTIONS & WAVEFORMS

Terrain Following, Terrain Avoidance. The next example is terrain following, terrain avoidance (TF/TA) shown in Figure 5.25. In terrain following (TF), the antenna scans several vertical bars oriented along the aircraft velocity vector and generates an altitude-range profile that is sometimes displayed to the pilot on an E-scan display. Depending on the aircraft's maneuvering capabilities, there is a control profile 1g acceleration maneuver control line shown as an upward curving line in the upper right of Figure 5.25.[86–88] If this conceptual line intercepts the terrain anywhere in range, an automatic up maneuver is performed. There is also a conceptual pushover line, not shown in the figure, which causes a corresponding down maneuver. The control profile in modern aircraft is automatic because a human pilot does not have the reflexes to avoid all possible detected obstacles.

In terrain avoidance (TA), the antenna scan is in a horizontal plane (shown in the upper left of Figure 5.25). Several altitude plane cuts are estimated and presented to

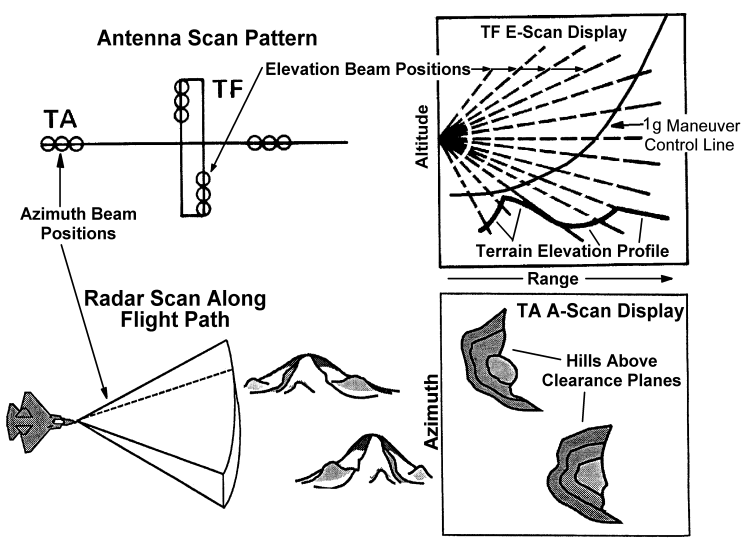

FIGURE 5.25 TF/TA mode example (*adapted*[8]*; courtesy SciTech Publishing*)

the pilot on an azimuth-range display (shown in the lower right of Figure 5.25). The terrain avoidance scan pattern shows all the terrain that is near or above the flight altitude and one cut below at a set clearance altitude (500 ft. typically).[86] Figure 5.25 (lower left and lower right) shows the situation geometry of an aircraft flying toward two hills and the corresponding altitude cuts displayed to the pilot. This allows either manual or automatic turning flight to maintain a lower altitude.

TF/TA allows an aircraft to penetrate at low altitude using the terrain as masking, thus preventing early detection. TF/TA is an important aspect of stealth even when the altitude is not all that low because lower altitudes provide some terrain obscuration and many other competing targets with similar cross-sections.[8]

Terrain Height Estimation. Some of the features of TF/TA are the required scan pattern, the number of independent frequency looks required to obtain a valid estimate of the height of a possibly scintillating object along the flight path, and the range coverage. Because terrain height is estimated through an elevation measurement, angle accuracy is critical. The range coverage, although short, requires multiple overlapping beams and multiple waveforms. One method for calculating terrain height[8] is shown in Figure 5.26. It consists of measuring the centroid and extent of each individual beam position over many pulses and estimating the top of the terrain in each beam, as shown in the figure. The calculation is summarized in Eq. 5.3.

$$P_r = \sum_i |S_i|^2 \text{ power received, } C_r = \text{Re}\left\{\frac{\sum_i S_i \times D_i}{P_r}\right\} \text{centroid}$$
$$E_r^2 = \frac{\sum_i |D_i|^2}{P_r} - C_r^2 \text{ extent squared, } T = C_r + 0.5 \times E_r \text{ terrain top estimate} \tag{5.3}$$

where S_i is a single sum monopulse measurement, D_i is the corresponding elevation difference monopulse measurement.

Usually the range-elevation profile is measured in multiple segments with separate PRFs and pulsewidths. The lowest PRF is used to measure the longest-range portion of the profile at the top of the elevation scan. It uses the largest pulse compression ratio (16:1–32:1). Each beam position overlaps by as much as 90% and multiple frequency

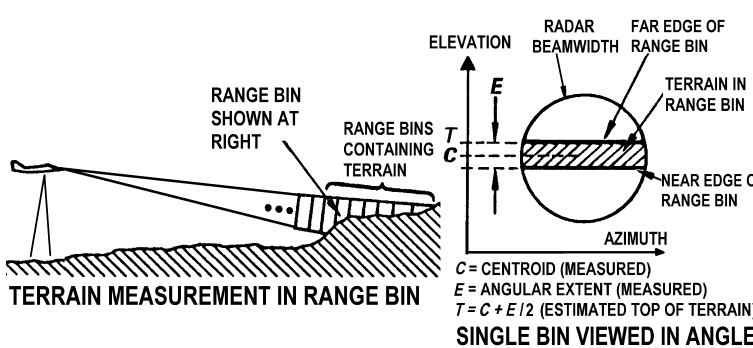

FIGURE 5.26 Terrain height estimation[8] (*Courtesy SciTech Publishing*)

looks in each beam create as many as 64 independent looks. The shortest range at the bottom of the elevation scan uses a short pulse with no pulse compression and a much higher PRF, but the same number of looks. The pulses in a T_{OT} are all the pulses that illuminate a single spot from the overlapping beams. Each overlapping beam must be compensated for the antenna look angle before the beams can be summed for a terrain height estimate from all the beams.[8] The radar cross section of the terrain could be quite low (e.g., snow-covered level treeless terrain), so some pulses may be integrated coherently to improve signal-to-noise ratio for a CPI of up to 8 pulses, as shown in the TF/TA entry in Table 5.1.

Terrain Database Merging. For the purposes of safety as well as stealth, active radar measurements are merged with a prestored terrain database.[87] Figure 5.27 shows the general concept of merged TF/TA measurements with stored data.

Active radar measurements are made out to a few miles. The instant use terrain database extends out to perhaps ten miles. The terrain database cannot be completely current and may contain certain systematic errors. For example, the database cannot contain the height of wires strung between towers or structures erected since the database was prepared. For the lowest possible flight profiles with less than 10^{-6} probability of crash per mission, the prestored data is merged and verified with active radar measurements. Low crash probabilities may also require some hardware and software redundancy. In addition, as the aircraft flies directly over a piece of terrain, combined terrain profile is verified by a radar altimeter function (TERCOM/TERPROM) in the RF and processor complex. Usually the prestored data is generated at the required resolution before a mission from the worldwide digital terrain elevation database (DTED).

Sea Surface Search, Acquisition, and Track. Sea surface search, acquisition, and track are oriented toward three types of targets: surface ships, submarines snorkeling or near the surface, and search and rescue. Tracking may be preliminary to attack with antiship weapons. Although most ships are large radar targets, they move relatively slowly compared to land vehicles and aircraft. In addition, sea clutter exhibits both current and wind-driven motion as well as "spiky" behavior. These facts often require high resolution and multiple looks in frequency or time to allow smoothing of sea clutter for stable detection and track.[16,45] If the target is a significant surface vessel, then RCS might be 1000 m^2, and a 30 m range resolution might be used for search

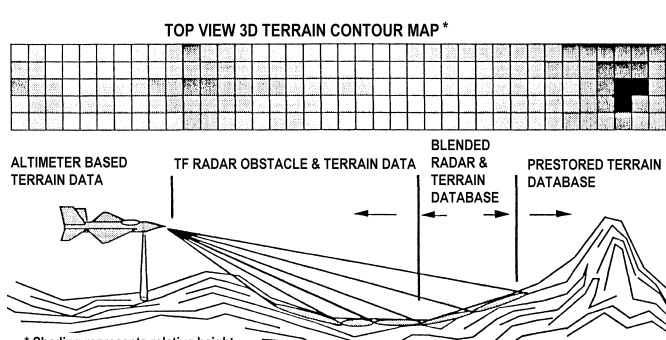

FIGURE 5.27 TF/TA terrain merging[7,8,87] (*Courtesy SciTech Publishing*)

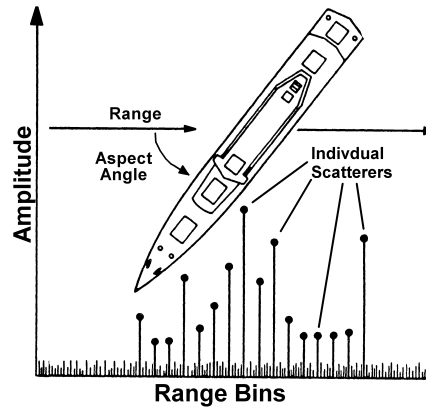

FIGURE 5.28 Range profile ship recognition[45]

and acquisition. If the target is a periscope or person in a life raft then 0.3 m resolution might be used since the RCS might be less than 1 m^2 and smoothing is especially important. DPCA and doppler processing is often interleaved with traditional bright (20 dB or greater above background) target detection. Lower PRFs are usually used, which imply relatively high pulse compression ratios, as shown in Table 5.1. Scan rates are often slow with one bar taking 10 seconds.

A high range resolution profile can be used to recognize a ship just as with an aircraft.[72] It naturally has the same weakness previously mentioned, and the aspect or attitude must be known. If the attitude is known, then the major scatterers can be mapped into a range profile and correlated with the ship power return in each cell. An example of a ship range profile is shown in Figure 5.28. These profiles are usually generated in track when the profile is stabilized in range.

The wake of a surface ship or submarine near the surface provides a substantial cross section over time but requires surface stabilized integration over 10–100s of seconds.[16,45] Earth's surface stabilized integration can be done using a motion compensated doppler beam sharpening (DBS) mode.

Inverse SAR. A far more reliable method of ship recognition is inverse synthetic aperture radar (ISAR).[16,72] The basic notion is that the motion of a rigid object can be resolved into a translation and rotation with respect to the line of sight to the target. The rotation gives rise to a differential rate of phase change across the object. The phase history differences can be match filtered to resolve individual scatterers in a range cell. Conceptually, such a matched filter is no different than a filter used to match a phase-coded pulse compression waveform. This is the basis of all SAR, RCS range imaging, observed geometric target acceleration, turntable imaging, and ISAR.

A ship in open water exhibits roll, pitch, and yaw motions about its center of gravity (c.g.). For example, Figure 5.29 shows a rolling motion of ± 2.3° that might be exhibited by a ship in calm seas. The roll motion might have a period of 10 seconds. The motion of almost all the scatterers on a large combatant are moving in arcs of circles projected as segments of ellipses to a radar observer.[45] For a radar observer the change in range, dR, associated with a roll movement is a function of the height, *h*,

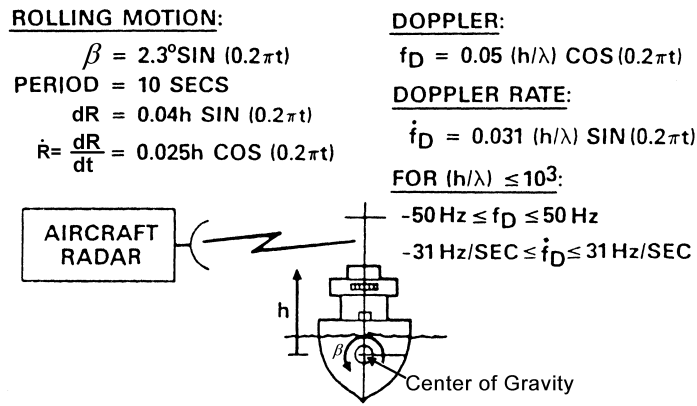

FIGURE 5.29 Inverse SAR notion[45]

of the scatterer above the center of gravity. The approximate range rate for each scatterer in rolling (pitch, yaw) motion at a height, h, is the time derivative of R shown in Figure 5.29. For a given desired cross range resolution with reasonable sidelobes, Δr_c, β must be equal to $\Delta r_c/\lambda$. For the example, 5 ft cross range resolution is obtainable with a 10-second observation time. The corresponding doppler and doppler rates are also given in Figure 5.29.

For a ship whose principal scatterers are less than 85 ft above the center of gravity, the dopplers will be in the range of ± 50 Hz at X band with a rate of change of up to ± 31 Hz/s. As long as the image resolution is not too great, each range-doppler bin can be match filtered using the hypothesized motion for each scatterer and an image can be formed on the ship. Each range bin may contain multiple scatterers from the ship in a given roll plane, and they may be distinguished by their differing phase history. However, scatterers in the pitch axis at the same range and roll height cannot be separated. Although pitch and yaw motions are slower, they also exist and allow separation in other similar planes.

Reasonably good images coupled with experienced radar operators allow recognition of most surface combatants. Recognition aids using prestored ship profiles allow identification to hull number in many cases. An example of a single ISAR image of a landing assault ship is given in Figure 5.30. The radar in this case is illuminating

FIGURE 5.30 Single ISAR ship image[45]

the ship from the bow at 30 km and 6° grazing. The bright scatterers exhibit cross range sidelobes, which can be partially reduced by sensing large returns, then applying amplitude weighting and display compression, as has been done in this image. Integration of multiple ISAR images dramatically improves quality.

Air-to-Ground Ranging. Air-to-ground ranging is used most often for targeting of guns, dumb bombs, and missiles with short-range seekers against fixed or slow moving targets. The target is detected and designated in some other mode such as GMTI, DBS, SAR, or SSS. The designated target is tracked in range and angle to provide a more accurate distance and angle to the target. The tracking may be open or closed loop. The estimates are then provided to the weapon before and after launch. Depending on distance, another designator, such as a laser, and the radar may be alternately slaved to one another. Both the radar and the other designator may be subject to atmospheric refraction, especially at low altitudes, which is sometimes estimated and compensated.

Precision Velocity Update. Precision velocity update (PVU) is used for navigation correction to an inertial platform. Although GPS updates are commonly used to provide navigation in many situations, a military aircraft cannot depend solely on its availability. Furthermore, inertial sensors are used to fill in between GPS measurements even under the best circumstances. Inertial sensors are extremely good over short span times, but velocity drift is a major long-time error source, e.g., 1 km/h accumulates 16.6 m error per minute. A radar mode may require position to 0.1 km for proper operation.

PVU generally uses three or more antenna beam positions in which it makes a velocity measurement, as shown in Figure 5.31.[15] This mode directly emulates dedicated radar doppler navigators. There is a three-stage velocity measurement process. First, the surface is automatically acquired in range. Second, a fine range measurement is made, often using monopulse discriminants and range centroiding similar to that shown in Eq. 5.3. Third, a line-of-sight velocity measurement, V_{LOS}, using doppler and/or range rate, is made also using centroiding. Because terrain may be rising or falling at the illuminated patches giving rise to velocity errors, terrain slope is estimated and used to correct the estimated velocity.

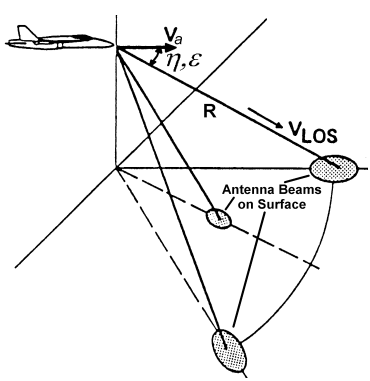

FIGURE 5.31 Precision velocity update concept[45]

A Kalman filter (a recursive filter that adaptively combines models of target measurements and of errors[10]) is employed to provide a better estimate of aircraft velocity. Although this procedure can be performed over land or water, sea currents make over-water measurements far less accurate. This velocity measurement provides in-flight transfer alignment of the various inertial platforms (aircraft, weapons, and radar). A set of outputs is provided to the mission management computer function, including North-East-Down (NED) velocity errors and estimates of statistical accuracies.

Sniff or Passive Listening. Most modes have a precursor subprogram called sniff, which looks for passive detections in a tentative operating channel before any radar emissions in that channel. The detections could be a friendly interferor, a jammer, or an inadvertent interferor such as a faulty civilian communications transponder.[99] This last example is the most common in the author's experience. It is not uncommon for a faulty transponder to appear as a million square meter target.

Doppler Beam Sharpening (DBS).[16,45,97] DBS is very similar to synthetic aperture radar (SAR) since both use the doppler spread across the antenna main beam to create higher resolution in the cross beam direction.[8,9,28,52] The principal difference is the amount of angular coverage, beam scanning, resolution, data gathering time, and accuracy of matched filtering in each range-doppler cell. A DBS map may take a second to gather over an angle of 70°. Depending on the angle from the aircraft velocity vector, a SAR map of a few feet resolution may take tens of seconds to gather at X band. DBS and SAR are compared in a qualitative way in Figure 5.32.

As the beam is positioned closer to the velocity vector, the doppler spread is smaller and so coherent dwell times must increase for the same resolution. Usually, there is a transition from shorter coherent processing intervals (CPIs) and longer post detection integrations (PDIs) to longer CPIs and shorter PDIs as the beam approaches the aircraft velocity vector. Near nose-on dwell times become prohibitive and the scan center is filled with real beam mapping. The real beam uses the same range resolution, but because returns from the entire beam are used, some amplitude equalization is required to provide uniform contrast and brightness across the whole map. Some effort is made

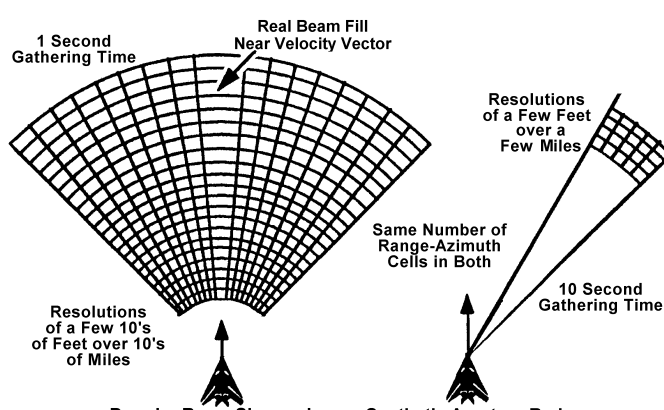

FIGURE 5.32 Doppler beam sharpening (DBS) comparison to SAR[9]

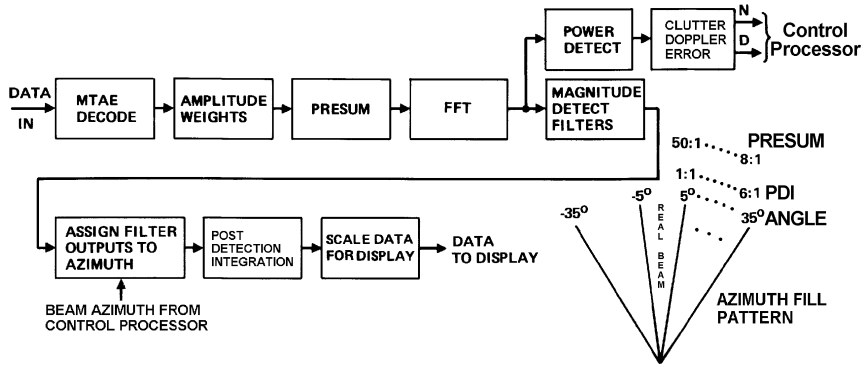

FIGURE 5.33 DBS processing (*adapted*[8]*; courtesy SciTech Publishing*)

to match filter (both in range closure and phase history) the doppler spread since iso-range and iso-dopplers are not close to orthogonal near the aircraft velocity vector (see Figure 5.8). SAR, on the other hand, is usually fully matched (relative to the desired resolution and phase history) in every range-doppler cell.

Figure 5.33 shows the signal processing that might be found in DBS mode. It consists of multiple time around echo (MTAE) suppression, amplitude weighting to improve sidelobes, presummation, an FFT filter bank, magnitude detection in each usable filter output, placement of each filter output in the correct ground stabilized location followed by post detection integration, and scaling for the display for constant brightness and dynamic range. Depending on grazing angle, ambiguous returns may compete with the region to be imaged. Often, a combination of sensitivity time control (STC) and pulse to pulse phase coding is used to reject multiple time around echoes (MTAE).[8,16,62,63] The amount of presummation (PRESUM) and post detection integration (PDI) as a function of beam position off the velocity vector is shown in the lower right of Figure 5.33. For each different angle, there is a different doppler spread across the beam. Therefore, in order to maintain a constant beam-sharpening ratio, different amounts of presumming must be used for each beam position. *Presumming* is the formation of an unfocussed synthetic beam (i.e., there is little or no attempt to match the exact phase history of surface points) inside the real antenna beam by what is essentially a lowpass filter. This would result in different target brightness and contrast if it were not compensated by applying a corresponding post detection integration (PDI) for each angle, as shown in Figure 5.33.

Multiple frequency looks are used to reduce speckle in the image and so several different frequencies are PDIed. The CPI is the presum ratio times the number of filter samples (128–800 is typical). Each CPI may have minor changes in the PRF to simplify processing and compensate for aircraft maneuvers. The aircraft may travel 1000 ft during the gathering time. There is considerable transport delay in most SAR and DBS processing; as a result, processed returns must be rectified (i.e., compensated for geometric distortion), motion compensated, and mapped into the proper space angle and range position. Since DBS usually maps a large area to provide overall ground situational awareness, the total range coverage is often covered in multiple elevation beams and range swaths. This is transparent to the operator but requires different PRFs, pulsewidths, filter shapes, and dwell times.

Although an MFAR contains a very stable time reference, uncertainties in the rate of change of terrain height, refraction, winds aloft, and very long coherent integration times force the measurement of the clutter doppler error versus predicted frequency to maintain proper focus and bin registration, as shown in the upper right in Figure 5.33. A similar function is performed in SAR as well.

Synthetic Aperture Radar. As is the case for DBS, SAR is a multirate-filtering problem, i.e., a cascade of filters in which the input sampling rate is higher than the output sampling rate, as shown in Figure 5.35, which requires very careful attention to range and azimuth filter sidelobes. Typically, the spacing of individual pulses on the ground is chosen to be much closer than the desired ultimate resolution. This allows linear range closure and phase correction since each point on the surface moves a significant fraction of a range cell pulse to pulse.[38,40–42,66,69,91] The input signal, point A in Figure 5.34, is shown as a spectrum at A, folded about the PRF on the left in Figure 5.35.

Subsequently, presummation is applied, which forms an unfocussed synthetic beam or filter inside the main-beam ground return (point B in Figure 5.34), which improves azimuth sidelobes and narrows the spectrum, as suggested in the center graph shown in Figure 5.35. The presummer output is resampled at a lower rate, f_S, consistent with acceptable filter aliasing. Then, range pulse compression is performed, assuming the transmitted pulse is very long compared to the range swath. If chirp (linear FM) is used, part of the "stretch" pulse compression processing is performed in the range compression function with the remainder performed in polar format processing. The dechirped and partially filtered or compressed output, shown at point C in Figure 5.34, may be resampled again at a new f_S, as indicated in the right graph shown in Figure 5.35, point C. In any case, azimuth variable phase adjustment and bin mapping (which compensates for changes in measurement space angles and range closure since significant motion occurs during the data gathering time) must be performed before azimuth filtering (sometimes called compression because it is similar to phase matched pulse compression). The output of azimuth compression is shown at point C. The complex SAR output map must be checked for depth of focus and usually requires autofocus since both atmospheric effects and locally rising or falling terrain may cause defocusing. Subsequent to refocusing, the map is magnitude detected and histogram averaged to maintain uniform brightness. The map is integrated with other looks, which requires

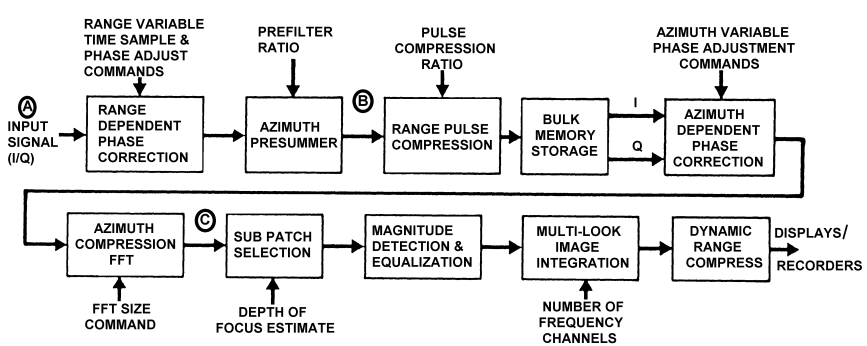

FIGURE 5.34 SAR processing (*adapted*[8]*; courtesy SciTech Publishing*)

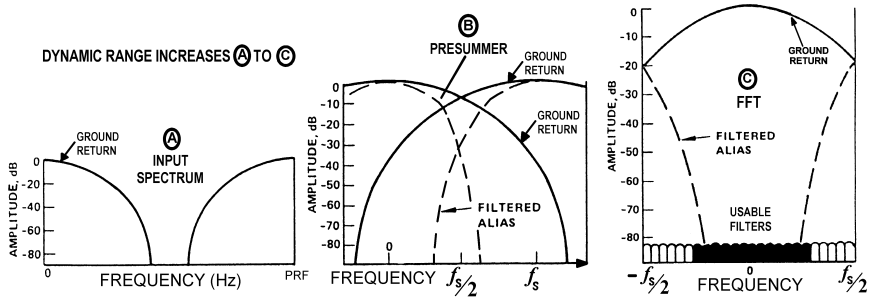

FIGURE 5.35 SAR Multirate Filtering (*adapted*[8]*; courtesy SciTech Publishing*)

geometrical correction and motion compensation. The total map dynamic range can easily be greater than 60 dB. The typical cockpit display is limited to 15–25 dB and dynamic-range compression, such as converting map amplitudes into their logarithms, is often performed.

DBS or SAR PRF, Pulse Length and Compression Selection. For each SAR or DBS geometry, the transmitted pulse width, pulse repetition interval, and pulse compression ratio must be calculated. One possible set of selection criteria is given in Eq. 5.4.[45]

Usually, the last range ambiguity before the range swath is chosen to be outside the main beam, far enough to be at least 20 dB down, including R^4 effects. Often in SAR, the transmitted pulse is much larger than the range swath, R_{swath}. Clearly, in each of the cases, the nearest integral clock interval and nearest convenient pulse compression ratio is selected because the values in Eq. 5.4 will be clock integers only by coincidence.

Pulse Repetition Interval (*PRI*):

$$\frac{\lambda}{2 \times V_a \times U_0 \times B_{\text{az}} \times \sin(\theta)} \geq PRI \geq \frac{2 \times (R_1 - R_{\min} + R_{\text{swath}} + R_p)}{c}$$

Pulse Width: $R_p \leq \text{Duty}_{\max} \times PRI \times c$
Minimum Allowable Ambiguous Range:
$R_{\min} \approx h \times \csc(\varepsilon + U_1 \times B_{\text{el}}/2)$
Range Swath is Geometry and Instrumentation Dependent:
$R_{\text{swath}} \leq h \times [\csc(\varepsilon - B_{\text{el}}/2) - \csc(\varepsilon + B_{\text{el}}/2)]$
and $R_{\text{swath}} \leq R_{\text{maxswath}}$ (5.4)

where: λ is transmitted wavelength, h is the aircraft altitude,
B_{az} & B_{el} are the azimuth & elevation half power beamwidths,
θ & ε are the angles between the velocity vector and antenna beam center,
R_1 is the distance to the first range bin, V_a is the aircraft velocity,
R_{swath} is the range swath length, R_{maxswath} is maximum instrumented range swath,
$R_{\min}$ is the range to the closest allowable ambiguity, $\text{Duty}_{\max}$ is allowable duty ratio,
R_p is the transmitted pulse length in distance units, c is the velocity of light,
U_0, U_1 are beamwidth multipliers at predefined power rolloff.

For example, assume $V_a = 300$ m/s, $\lambda = 0.03$ m, $h = 5000$ m, $\theta = 0.5$, $\varepsilon = 0.1$, B_{az}, $B_{el} = 0.05$, U_0, $U_1 = 2.3$, $R_{swath} = 2$ km, $R_{min} = 32$ km, desired mapping range, $R_1 = 50$ km, $\text{Duty}_{max} = 0.25$, selecting a first guess for $R_p = 8000$ m; then $186 < PRI < 906$ μsec, R_{min} is the equivalent of 213 μsec, and the next allowable ambiguity would be past the swath at 400 μsec; therefore, a PRI of 213 or 400 μsec could be used with a transmitted pulse of approximately 50 or 100 μsec respectively.

Ground Moving Target Indication (GMTI) and Track (GMTT). GMTI is the detection and acquisition of ground moving targets. GMTI and GMTT radar modes have a different set of challenges. First, target detection is usually the easy part; the RCS of most anthropogenic objects and many natural moving targets is large (10–1000 m^2). Unfortunately, there are many stationary objects with moving parts such as ventilators, fans, water courses, and power lines that lead to apparent false alarms.[93] Often slow-moving vehicles have fast-moving parts (e.g., helicopters and agricultural irrigators).

Most areas have large numbers of vehicles and scatterers that could be vehicles. It is typical to have up to 20,000 bona fide GMTs in the field of view. Processing capacity must be adequate to handle and discriminate thousands of high *SNR* threshold crossings and hundreds of moving targets of interest. Usually multi-hypothesis tracking[10] filters will be following several hundred GMTs of interest simultaneously. In most cases, all targets must be tracked and then recognized on the basis of doppler spectrum (helicopters vs. wheeled vehicles vs. tracked vehicles vs. scanning antennas), rate of measured location change (ventilator locations don't change), and consistent trajectory (e.g., 60 mph where there are no roads is improbable for a surface vehicle).[94] In addition, vehicles of interest may have relatively low radial velocities requiring endoclutter processing[16] (i.e., far enough inside main-beam clutter that detection is limited for doppler only filtering).

A processing block diagram for GMTI is shown in Figure 5.36. Although there are alternate ways to perform endoclutter processing, a multiple phase center–based

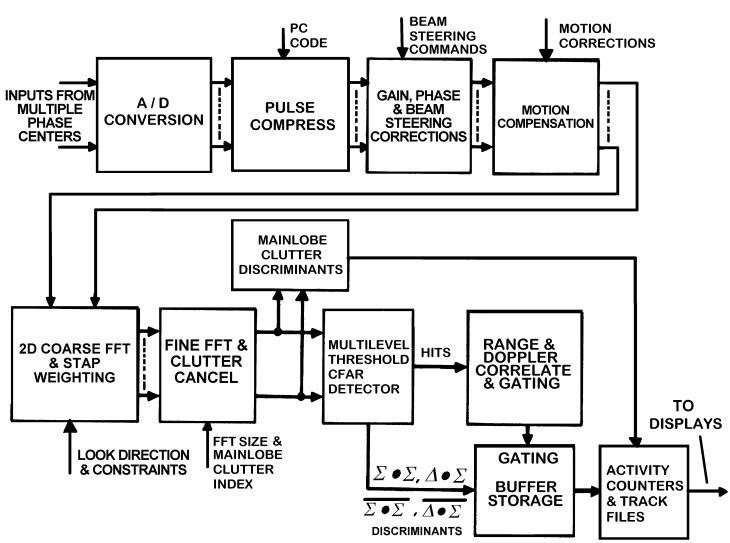

FIGURE 5.36 Ground moving target detection processing (*adapted*[8]*; courtesy SciTech Publishing*)

processing scheme is given in Figure 5.36. Multiple channels or phase centers are digitized and pulse compressed. Periodic calibration signals are used to create a gain, phase and beam steering correction table for all frequencies, antenna beam steering, and channels, which are then applied to the digitized measurements in each channel. Motion compensation to a fraction of a wavelength for platform maneuvers or deviations is applied to the data. A coarse two-dimensional FFT is performed followed by space-time adaptive calculations, and filter weighting is applied to reject some clutter and jamming. High resolution doppler filtering is performed in a conventional FFT,[90,96,97] perhaps with DPCA clutter cancellation. Doppler filter outputs are used to form main-beam clutter error discriminants for precisely measuring doppler center frequency to provide fraction of wavelength motion compensation. Main-beam clutter is not in the same frequency location for each range bin, and so filter output order must be adjusted to present a common input to the threshold detector. The doppler filter bank outputs also are applied to a multilevel threshold detector for ground moving target detection similar to those described in "Ground Moving Target Thresholding." Sum and difference discriminant functions are formed and stored in buffer storage for each detected moving target to improve target tracking and geolocation accuracy.

Often PRFs are ambiguous in both range and doppler but unambiguous inside the main beam and near sidelobes (i.e., there is only one range or doppler ambiguity interval in the main beam and near sidelobes). PRF selection is similar to A-A MPRF. Usually fewer PRFs are used; four or five are typical.[97] A range ambiguity may be in the main beam at low grazing angles. Two out of four or three out of five is usually the final detection criteria. PRFs typically are 4–8 kHz. Coded waveforms are often used to reject ambiguous returns outside the antenna main beam that compete with the region of interest. A 10 ft range cell size is often used to match the smallest vehicle of interest and to reduce background clutter. Ground moving target recognition may require 0.25 ft resolution. Antenna illumination must be ground stabilized since the aircraft will engage in both intentional and unintentional maneuvers.[94]

Ground Moving Target Thresholding. The typical multilevel threshold has several unique features. In addition to the obvious alert-confirm properties (a double thresholding method in which a lower first threshold nominates radar returns as possible targets to be confirmed by a return observation with a higher threshold), it also uses multiple phase center discriminants as well as near sidelobe threshold multipliers.[94] Even with STAP, the non-gaussian nature of clutter requires higher thresholds in the main beam and near sidelobes.[98] Threshold crossings are correlated in range and doppler and buffered along with corresponding phase center discriminants, which are presented to tracking filters or activity counters.

There are three regions of thresholding: main-beam clutter-limited detection, near sidelobe clutter-limited detection, and thermal-noise-limited detection. Near surface targets of interest will often have radial velocities of a few miles per hour for long periods of time, which forces the detection of ground moving targets well into main-beam clutter. Phase monopulse, DPCA, or STAP processing allows the first order cancellation of clutter for many slow-moving targets. Unfortunately, clutter does not always have well-behaved statistical tails, and to maintain a constant false alarm rate, the threshold must be raised for endoclutter targets. The output of the doppler filter bank might be thought of as a two dimensional range-doppler image. There will still be parts of main-beam clutter that are completely discarded except for motion compensation because clutter cancellation is inadequate.[98]

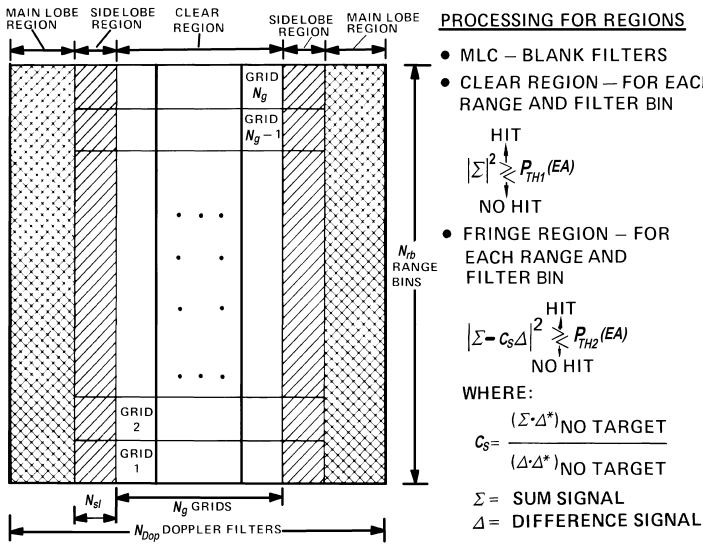

FIGURE 5.37 Multiregion GMT thresholding[8] (*Courtesy SciTech Publishing*)

An example thresholding scheme based on these concepts is shown in Figure 5.37. The range-doppler space is broken up into a grid of range bins and doppler filters, as shown in the figure. Each cell in the grid might be 64 × 64 range-doppler bins with 256 grid cells total. Some grid locations close to main-beam clutter (MLC in figure) are used for forming main-beam clutter discriminants only and are otherwise discarded. The bins (64^2 in the example) in each grid cell are ensemble averaged (EA) in sum and difference channels. The power in each bin in a grid cell in the clear (thermal noise limited) region is compared to a threshold, $P_{TH1}(EA)$, which is a function of the EA in that grid cell. In the endoclutter near sidelobe region, a discriminant, C_s, is formed and used to provide additional clutter cancellation prior to thresholding. Again, the threshold, $P_{TH2}(EA)$, is a function of the EA in that grid cell and a priori knowledge of the clutter statistics. Although only one threshold is described, two are actually used before hits and their corresponding discriminants are passed to the track files. All low threshold hits are passed to activity counters. As complex as this thresholding scheme seems to be, it is very detection power efficient.

Typical GMT Weapon Delivery. As mentioned previously, missile guidance requires tracking of both targets and missiles (also bullets in gun laying radar; *gun laying* is a term invented by the U.K during WWII for radar pointing of antiaircraft guns). Range accuracy is at least an order of magnitude better than angle accuracy. Some method must be used to improve angle accuracy for weapon delivery. An example processing diagram for GMT weapon delivery is shown in Figure 5.38. In this case, three different classes of target or missile are tracked. A single waveform may be used to track stationary, endo- and exoclutter moving targets, and missiles or bullets. Each class of return, based on its range and doppler location, is separately tracked and geolocated.[94]

There are several common types of geolocation; many of them are based on using either DTED or cartographic data. One method using cartographic data is shown

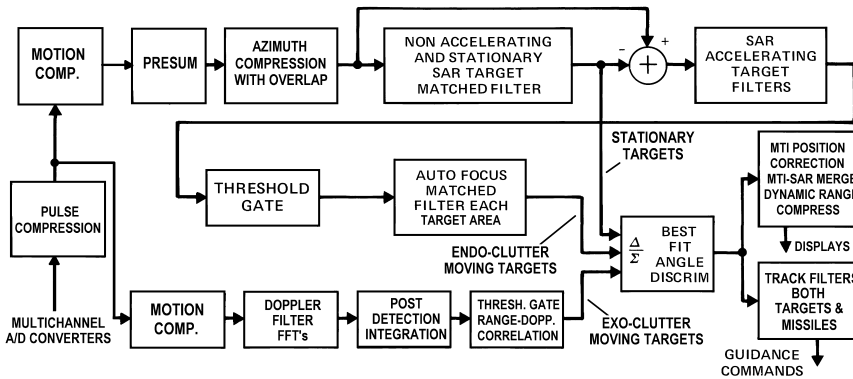

FIGURE 5.38 Typical GMT weapon guidance (*adapted*[8]*; courtesy SciTech Publishing*)

in Figure 5.39. An error ellipse and its corresponding eccentricity are calculated for each target. If the eccentricity is less than some arbitrary threshold (e.g., 0.866 relative), the minimum perpendicular distance is calculated for road segments inside the 3-sigma ellipse. As shown in the figure, the perpendicular intercept may not lie inside the road segment and will be discarded. The minimum distance for valid road segment distances will be selected as the GMT location. If the eccentricity is greater than the threshold, the road segments that have a major ellipse axis intercept inside 3 sigma are compared, and the minimum distance is selected. Obviously, some other screening must also be applied. For example, some roads cannot support high speeds and tanks do not have to be on roads.

A common SAR-MTI display may be presented to the operator. In addition, guidance commands or errors are derived from the measurements and provided to downlinks to either missiles on the fly or gun directing computers for the next rounds. Short-term coherent change detection may be used to separate stationary targets from slow-moving endoclutter targets. Short-term coherent change detection is a method in which two coherent SAR maps taken within a few hours of one another at the same frequency are registered and cross-correlated pixel by pixel. The fast-moving target category usually includes both targets and bullets or missiles.

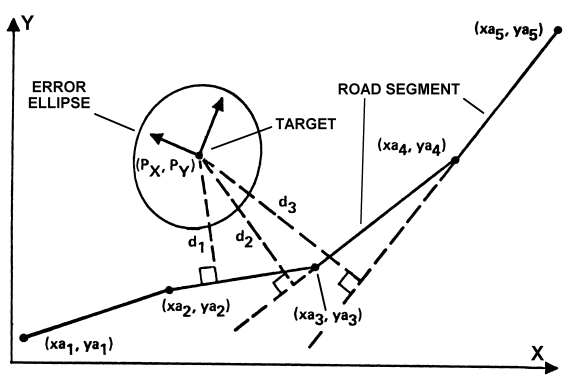

FIGURE 5.39 Cartographic-assisted GMT geolocation[94]

Missile Performance Assessment, Track, and Update. Missile midcourse guidance usually consists of assessing the missile performance, measurement of the target and missile location, prediction of the path of each, and updating the resulting data to the missile for the best future intercept of the target. It may also include the most current estimate of the target type and attitude for best fuzing. The missile usually sends data about its state of health, ownship measurements, remaining fuel amounts, and target acquisition, if any.[74] When the missile is close to the data link aircraft (which may or may not be the launching platform), communication is often through an aperture other than in the main MFAR. As the distance gets greater, the primary MFAR aperture is used. As the data link aircraft maneuvers, the aperture that has the largest projected area in the direction of the missile is used. The bandwidth to the missile is very low and can be redundant and highly encrypted to provide good antijam (A/J) protection. If it contains imagery, the uplink bandwidth from the missile is relatively large and will have comparatively lower A/J performance. An adaptive MFAR primary aperture can improve a wider band missile uplink A/J if the jammer is offset from the target. At the missile end, the missile antenna can have jammer nulling to improve downlink A/J.[43,85]

AGC, Calibrate and Self-Test. Usually at the beginning of a new mode, the end of each scan bar, or once per second, the calibrate and self-test subprogram is invoked by the operational flight program (OFP) executive. A sequence of subroutines is executed that measures phase and gain unbalance between channels using a signal injected on the antenna. This is usually done over a range of input amplitudes, frequencies, and AGC settings because of the nonlinear characteristics of most RF front ends. Also for modes like TF/TA, a full set of off-angle diagnostics is performed, which tests the integrity of the entire measurement, processing, and flight control chain often enough to keep the probability of a failure-induced crash per flight below 10^{-6} in the presence of jamming or component failures.

In addition, there are initiated built-in tests at two levels: an operational readiness test performed as part of mission initiation and a fault isolation test performed by the maintenance crew in response to an operator deficiency report. Both tests take longer and are more exhaustive. In the best case, the specific flight line or a first-level maintenance replaceable assembly is identified with high probability. Such assemblies are then sent to a depot for replacement, repair, failure tracking, and/or reclamation. For assemblies that have a very low failure rate, it is usually cheaper to replace and reclaim rather than repair even when the assembly is very expensive.

REFERENCES

Short course notes and other papers can usually be obtained from the authors or the course sponsor for a small fee. All of the authors' papers referenced are available in Adobe Acrobat format subject only to copyright restrictions by e-mail request: davidlynchjr@ieee.org and carlo.kopp@iinet.net.au.

1. C. Kopp, "Active electronically steered arrays," 2002, http://www.ausairpower.net.
2. Joint Advanced Strike Technology Program, "Avionics architecture definition 1.0," U.S. DoD public release, unlimited distribution and use, pp. 9, 11, 31,32, 1994.
3. D. Eliot (ed.), *Handbook of Digital Signal Processing*, San Diego, CA: Academic Press, 1987, pp. 364–464, 527–589, 590–593, 594–631.
4. L. Tower and D. Lynch, "Pipeline High Speed Signal Processor," U.S. Patent 4,025,771, 5/24/1977.

5. L. Tower and D. Lynch, "System for Addressing and Address Incrementing of Arithmetic Unit Sequence Control System," U.S. Patent 4,075,688, 2/21/1978.
6. L. Tower and D. Lynch, "Pipelined microprogrammable control of a real time signal processor," in *IEEE Micro6 Conference*, June 1973, p. 175.
7. D. Lynch, "Radar systems for strike/fighter aircraft," presented at *AOC Third Radar/EW Conference Proceedings*, Unclassified paper in classified proceedings available from author by request, February 12–13, 1997.
8. D. Lynch, *Introduction to RF Stealth,* Raleigh, NC: SciTech Publishing, 2004, pp. 446–451, 82–84, 198–221, 467–470 492–501, 504–531.
9. D. Lynch et al., "Advanced avionics technology," Evolving Technology Institute Short Course Notes, November 1994.
10. S. S. Blackmun, *Multiple Target Tracking with Radar Applications*, Dedham, MA: Artech House, 1986, pp. 25–44, 281–298.
11. D. A. Fulghum and D. Barrie, "Radar becomes a weapon," *Aviation Week & Space Technology*, pp. 50–52, September 5, 2005.
12. Image Courtesy Raytheon Company, cleared for public release, 265-SPR127.05.
13. M. Streetly, *Radar and Electronic Warfare Systems*, 1999–2000, 11th Ed., Coulsdon, Surrey, UK: Janes Information Group, 1999, pp. 250–254.
14. R. Nitzberg, *Radar Signal Processing and Adaptive Systems*, Norwood, MA: Artech House, 1999, pp. 199–202, 207–236, 267–290.
15. W. K. Saunders, "CW and FW radar"; F. M. Staudaher, "Airborne MTI"; W. H. Long, D.H. Mooney, and W. A. Skillman, "Pulse doppler radar"; R. J. Serafin, "Meteorological radar," *Radar Handbook*, 2nd Ed., M. Skolnik (ed.), New York: McGraw Hill, 1990, pp. 14.37–14.39, 16.8–16.28, 17.33–17.35, 23.5–23.13.
16. P. Lacomme, J-P. Hardange, J-C. Marchais, and E. Normant, *Air and Spaceborne Radar Systems: An Introduction*, Norwich, NY: William Andrew Publishing, 2001, pp. 329–335, 371–425, 171–176, 469.
17. J. Davis, "Sun intros eight–core processor," *Electronic News*, Reed Elsevier, November 14, 2005.
18. Altera Corporation, "Stratix II FPGA's," November 2005, http://www.altera.com.
19. D. A. Fulghum, "Deep look," *Aviation Week and Space Technology*, January 17, 2005.
20. D. A. Fulghum, "Future radar," *Aviation Week and Space Technology*, October 4, 2004.
21. M. Peck and G. W. Goodman, Jr., "Agile radar beams," *C4ISR Journal*, pp. 22–28, May 2005.
22. "Raytheon's APG-79 AESA radar for the F/A-18 Super Hornet sets a new standard as it delivers multiple JDAMs simultaneously on target," *MarketWatch*, December 5, 2005.
23. M. Selinger, "U.S. Navy eyes 'growth plan' for Super Hornet's AESA radar," *Aerospace Daily and Defense Report*, December 6, 2005.
24. R. E. Hudson, S. O. AKS, P. P. Bogdanovic, and D. D. Lynch, "Method and System for Reducing Phase Error in a Phased Array Radar Beam Steering Controller, U.S. Patent 4,924,232, 5/8/1990.
25. R. Hill, D. Kramer, and R. Mankino, "Target Detection System in a Radar System Employing Main and Guard Channel Antennas," U.S. Patent 3875569, 4/1/1975.
26. R. Monzingo and T. Miller, *Introduction to Adaptive Arrays*, New York: John Wiley & Sons, 1980, pp. 78–279.
27. R. Klemm, "Adaptive airborne MTI: An auxiliary channel approach," *IEE Proceedings*, vol. 134, part F, no. 3, p. 269, 1987.
28. S. Aks, D. D. Lynch, J. O. Pearson, and T. Kennedy, "Advanced modern radar," Evolving Technology Institute Short Course Notes, November 1994.
29. Work performed by L. Griffiths and C. Tseng, "Adaptive array radar project review," Hughes Aircraft IR&D, performed at USC, July 18, 1990.
30. C. Ko, "A fast adaptive null-steering algorithm based on output power measurements," *IEEE Transactions on Aerospace and Electronic Systems*, vol. 29, no. 3, pp. 717–725, July 1993.

31. H. Wang, H. Park, and M. Wicks, "Recent results in space-time processing," in IEEE National Radar Conference 1994, pp. 104–109.
32. J. Ward, "Space-time adaptive processing for airborne radar," MIT Lincoln Laboratory Report 1015, approved for unlimited public distribution.
33. N. M. Greenblatt, J. V. Virts, and M. F. Phillips, "F-15 ESA medium PRF design," Hughes Aircraft IDC No. 2312.20/804, January 9, 1987, unclassified report.
34. D. Schleher, "Low probability of intercept radar" in *IEEE International Radar Conference*, 1985, p. 346.
35. E. Carlson, "Low probability of intercept techniques and implementations," in *IEEE National Radar Conference*, 1985, p. 51.
36. Groger, "OLPI-LPI radar design with high ARM resistance," in *DGON 7th Radar Conference* 1989, p. 627.
37. D. Lynch, "Real time radar data processing," presented at IEEE Solid State Circuits 4.10 Committee, Digital Filtering Meeting, New York, October 30, 1968.
38. D. Craig and M. Hershberger, "FLAMR operator target/OAP recognition study," Hughes Aircraft Report No. P74-524, January 1975, Declassified 12/31/1987.
39. D. C. Schleher, *Electronic Warfare in the Information Age*, Norwood, MA: Artech House, 1999, pp. 279–288, 133–199.
40. S. Hovanessian, *Introduction to Synthetic Array and Imaging Radars*, Dedham, MA: Artech House, 1980, Chapter 5.
41. J. Curlander and R. McDonough, *Synthetic Aperture Radar Systems and Signal Processing*, New York: Wiley & Sons, 1991, pp. 99–124, 427–535.
42. J. Kovaly, *Synthetic Aperture Radar*, Dedham, MA: Artech House, 1976, pp. 72–79, 118–123, 249–271.
43. B. Lewis, F. R. Kretschmer, and W. W. Shelton, *Aspects of Radar Signal Processing*, Dedham, MA: Artech House, 1986, pp. 267–290.
44. M. Radant, D. Lewis, and S. Iglehart, "Radar sensors," UCLA Short Course Notes, July 1973.
45. D. Lynch, J. O. Pearson, and E. Shamash, "Principles of Modern radar," Evolving Technology Institute Short Course Notes, June 1988.
46. J. Frichel and F. Corey, "AN/APG-67 Multimode Radar Program," in *IEEE NAECON 1984*, p. 276.
47. R. Nevin, "AN/APG-67 multimode radar performance evaluation," in *IEEE NAECON 1987*, p. 317.
48. D. Lynch, "SLOSH filter processing," presented at IEEE AU Symposium on Digital Filters, Harriman, NY, January 1970.
49. Treffeisen et al., "Obstacle Clearance System for Aircraft," U.S. Patent 3,530,465, 9/22/1970.
50. *International Defense Review- Air Defense Systems*, Geneva, Switzerland: Interavia, 1976, pp. 61–103.
51. C. Kopp, "Missiles in the Asia-Pacific," *Defence Today*, http://www.ausairpower.net/DT-Missile-Survey-May-05.pdf.
52. G. Stimson, *Introduction to Airborne Radar*, 2nd Ed., Mendham, NJ: SciTech Publishing, 1998, pp. 355–381, 463–465, 431–437.
53. J. Clarke, "Airborne radar" Parts 1 & 2, *Microwave Journal*, p. 32 and p. 44, January 1986 and February 1986.
54. E. Aronoff and D. Kramer, "Recent developments in airborne MTI radars," Hughes Aircraft Report, presented at IEEE Wescon 1978.
55. D. Kramer and G. Lavas, "Radar System with Target Illumination by Different Waveforms," U.S. Patent 3866219, 2/11/1975.
56. D. Mooney, "Post-Detection STC in a Medium PRF Pulse Doppler Radar," U.S. Patent 4095222, 6/13/1978.
57. E. Frost and L. Lawrence, "Medium PRF Pulse Doppler Radar Processor for Dense Target Environments," U.S. Patent 4584579, 4/22/1986.
58. W. Long and K. Harriger, "Medium PRF for the AN/APG-66 radar," in *IEEE Proceedings*, vol. 73, no. 2, p. 301.

59. E. Aronoff and N. Greenblatt, "Medium PRF radar design and performance," Hughes Aircraft Report, presented at IEEE National Radar Conference 1975.
60. H. Erhardt, "MPRF processing functions-issue 2," Hughes Aircraft IDC, October, 18, 1977, unclassified report.
61. J. Kirk, "Target Detection System in a Medium PRF Pulse Doppler Search/Track Radar Receiver," U.S. Patent 4079376, 3/14/1978.
62. K. Gerlach, "Second time around radar return suppression using PRI modulation," *IEEE Transactions on Aerospace and Electronic Systems*, vol. AES-25, no. 6, pp. 854–860, November 1989.
63. L. Durfee and W. Dull, "MPRF Interpulse Phase Modulation for Maximizing Doppler Clear Space," U.S. Patent 6518917, 2/11/2003.
64. S. Hovanessian, "An algorithm for calculation of range in multiple PRF radar," *IEEE Transactions on Aerospace & Electronic Systems*, vol. AES-12, no. 2, March 1976, pp. 287–290.
65. G. Morris, *Airborne Pulse Doppler Radar*, Norwood, MA: Artech House, 1988.
66. R. Schlolter, "Digital realtime SAR processor for C & X band applications," in *IGARSS 1986*, Zurich, vol. 3, p. 1419.
67. R. Klemm, "Airborne MTI via digital filtering," in *IEE Proceedings*, vol. 136, part F, no. 1, 1989, p. 22.
68. Technology Service Corp., "Adaptar space-time processing in airborne radars," TSC-PD-061-2, February 24, 1971, unclassified report.
69. D. Lynch, "Signal processor for synthetic aperture radar," presented at SPIE Technical Symposium East 1979, paper no. 180-35.
70. J. Harmon, "Track before detect performance for a high PRF search mode," in *IEEE National Radar Conference* 1991, pp. 11–15.
71. J. R. Guerci, *Space-Time Adaptive Processing for Radar*, Norwood, MA: Artech House, 2003, pp. 6, 11–28, 51–74.3.
72. P. Tait, *Introduction to Radar Target Recognition*, Bodmin, Cornwall, UK: IEE, 2005, pp. 105–217, 317–347.
73. P. Peebles, *Radar Principles*, New York: John Wiley & Sons, 1998, pp. 318–349, 599–614.
74. E. Eichblatt, *Test and Evaluation of the Tactical Missile*, Washington, DC: AIAA, 1989, pp. 13–39, 52–54.
75. R. Macfadzean, *Surface Based Air Defense System Analysis*, self-published, 1992 & 2000, pp. 213–243.
76. M. Robin and M. Poulin, *Digital Television Fundamentals*, 2nd Ed., New York: McGraw-Hill, 2000, pp. 345–425.
77. W. Pratt, *Digital Image Processing*, New York: Wiley & Sons, 1978, pp. 662–707.
78. M. Simon, J. Omura, R. Scholtz, and B. Levitt, "Low probability of intercept communications," Chapter 4 in *Spread Spectrum Communications Handbook*, New York: McGraw-Hill, 1994, pp. 1031–1093.
79. W. Gabriel, "Nonlinear spectral analysis and adaptive array superresolution techniques," NRL Report 8345, 1979, approved for unlimited public distribution.
80. J. Asenstorfer, T. Cox, and D. Wilksch, "Tactical data link systems and the Australian defense force (ADF)-technology developments and interoperability issues," Defense Science and Technology Organisation Report, DSTO-TR-1470, approved for public release.
81. C. Kopp; "The properties of high capacity microwave airborne ad hoc networks," Ph.D. dissertation, Monash University, Melbourne, Australia, October 2000.
82. J. Katzman, *Defence Industry Daily*, http://www.defenseindustrydaily.com/2005/12/elec-tricks-turning-aesa-radars-into-broadband-comlinks/index.php.
83. C. Nakos, S. Baker, J. J. Douglass, and A. R. Sarti, "High speed data link," Australia Patent PCT/AU97/00255, WO 97/41450, DSTO Tactical Surveillance Systems Division, Salisbury, Australia, November 1997.
84. D. A. Fulghum, "See it, jam it, kill it" *Aviation Week & Space Technology*, pp. 24, 25, May 30, 2005.

85. D. C. Schleher, *Introduction to Electronic Warfare*, Dedham, MA: Artech House, 1986, pp. 280–283, 109–128.
86. Case, Jr. et al., "Radar for Automatic Terrain Avoidance," U.S. Patent 3,815,132, 6/4/1974.
87. H. L. Waruszewski, Jr., "Apparatus and Method for an Aircraft Navigation System Having Improved Mission Management and Survivability Capabilities," U.S. Patent 5,086,396, 2/4/1992.
88. Barney et al., "Apparatus and Method for Adjusting Set Clearance Altitude in a Terrain Following Radar," U.S. Patent 4,760,396, 7/26/1988.
89. R. Jaworowski, "Outlook/specifications military aircraft," *Aviation Week and Space Technology*, pp. 42–43, January 17, 2005.
90. F. Harris and D. Lynch, "Digital signal processing and digital filtering with applications," Evolving Technology Institute Short Course Notes, 1971–1983, pp. 366, 744–748, February 1978.
91. R. Fabrizio, "A high speed digital processor for realtime SAR imaging," in *IGARSS 1987*, Ann Arbor MI, vol. 2, p. 1323.
92. T. Cullen and C. Foss (eds.), *Janes Land-Based Air Defence 2001–2002*, Coulsdon, Surrey, UK: Janes Information Group, 2001, pp. 129–134.
93. R. Klemm, "New airborne MTI techniques," in *International Radar Conference London*, 1987, p. 380.
94. "Pave mover TAWDS design requirements," Hughes Aircraft Specification, November 1979, unclassified, unlimited distribution.
95. J. Pearson, "FLAMR signal to noise experiments," Hughes Aircraft Report No. P74-501, December 1974, declassified 12/31/1987.
96. E. O. Brigham, *The Fast Fourier Transform*, New York: Prentice Hall, 1974, pp. 172–197
97. D. Lynch, et al., "LPIR phase 1 review," Hughes Aircraft Report, 1977, unclassified report.
98. J. O. Pearson, "Moving target experiment and analysis," Hughes Aircraft Report No. P76-432, pp. 5–15, 22–35, December 1976, declassified 2/28/94.
99. K. Rogers, "Engineers unlock mystery of car-door device failures," *Las Vegas Review Journal*, August 19, 2004, p. 1B.